

ARMY RESEARCH LABORATORY



# An Analysis Comparison Using the Vulnerability Analysis for Surface Targets (VAST) Computer Code and the Computation of Vulnerable Area and Repair Time (COVART III) Computer Code

by David D. Lynch, Robert W. Kunkel,  
and Stephanie S. Juarascio

ARL-MR-341

February 1997

19970228 071

The findings in this report are not to be construed as an official Department of the Army position unless so designated by other authorized documents.

Citation of manufacturer's or trade names does not constitute an official endorsement or approval of the use thereof.

Destroy this report when it is no longer need. Do not return it to the originator.

# **Army Research Laboratory**

Aberdeen Proving Ground, MD 21005-5068

---

**ARL-MR-341**

**February 1997**

## **An Analysis Comparison Using the Vulnerability Analysis for Surface Targets (VAST) Computer Code and the Computation of Vulnerable Area and Repair Time (COVART III) Computer Code**

**David D. Lynch, Robert W. Kunkel, Stephanie S. Juarascio**  
Survivability/Lethality Analysis Directorate, ARL

---

---

## Abstract

---

A vulnerability analysis was performed on a missile launcher using the U.S. Army Research Laboratory's (ARL) aircraft vulnerability code, Computation of Vulnerable Area and Repair Time (COVART III). A subsequent analysis was also performed using the Vulnerability Analysis for Surface Targets (VAST) computer code, and the results compared. While only slight differences were noted in the view-averaged comparisons, significant differences were noted on a cell-by-cell level. This report documents the model comparison.

## TABLE OF CONTENTS

	<u>Page</u>
<b>LIST OF FIGURES</b> .....	v
<b>1. INTRODUCTION</b> .....	1
1.1 Objective .....	1
1.2 Approach .....	1
<b>2. EXPERIMENTAL SETUP</b> .....	2
2.1 General Observations .....	2
2.1.1 Ray-Tracing (Shotline) Techniques .....	4
2.1.2 Generating Inputs .....	4
2.1.3 $P_{k/h}$ Functions .....	5
2.1.4 Kill Definitions .....	5
2.1.5 Personnel Incapacitation .....	5
2.1.6 Special Caveats for Aircraft .....	5
2.1.7 Behind Armor Debris Modeling Capability .....	6
2.1.8 Repair Time Modeling Capability .....	6
2.1.9 Model Input Requirements and Format .....	6
2.1.10 Documentation .....	6
2.2 $A_v$ Comparisons .....	6
2.3 Cell-by-Cell $P_k$ Differences .....	8
2.4 Distribution of $P_k$ s by View .....	8
2.5 Average $P_k$ s by View .....	10
2.6 Comparison of COVART III and VAST Penetration Algorithms .....	11
2.6.1 COVART III Penetration Algorithms .....	11
2.6.2 VAST Penetration Equations (Steel Fragments) .....	14
2.6.3 Evaluation Along a Shotline Using COVART III .....	15
2.6.4 Evaluation Along a Shotline Using VAST .....	17
2.7 Summary of Differences .....	19
<b>3. CONCLUDING REMARKS</b> .....	20
<b>4. REFERENCES</b> .....	23
<b>APPENDIX A: HISTOGRAMS</b> .....	25
<b>APPENDIX B: VIEW-AVERAGED PROBABILITY OF KILLS (<math>P_k</math>s)</b> .....	45
<b>APPENDIX C: VULNERABILITY ANALYSIS FOR SURFACE TARGETS (VAST) MATERIAL CONSTANTS</b> .....	51

DISTRIBUTION LIST .....	55
REPORT DOCUMENTATION PAGE .....	59

## LIST OF FIGURES

<u>Figure</u>		<u>Page</u>
1.	Flow chart of a VAST kinetic energy (KE) fragment analysis process .....	3
2.	Flow chart of a COVART III KE fragment analysis process .....	3
3.	Plot of $A_v$ s calculated using VAST for a mobility kill .....	7
4.	Plot of $A_v$ s calculated using COVART III for a mobility kill .....	7
5.	$P_k$ histogram for a mobility kill given 5 grain, 5,000 fps steel fragment impact at 90° azimuth, 0° elevation .....	9
6.	$P_k$ histogram for a mobility kill given 120 grain, 5,000 fps steel fragment impact at 90° azimuth, 0° elevation .....	9

**INTENTIONALLY LEFT BLANK.**

## 1. INTRODUCTION

In fiscal year (FY) 1992, a vulnerability analysis of a missile launcher was performed using the Ballistic Vulnerability/Lethality Division's (BVLD's) aircraft vulnerability analysis code, Computation of Vulnerable Area and Repair Time (COVART III) (Joint Technical Coordinating Group for Munitions Effectiveness [JTCG/ME] [Anti-Air] 1985). In support of a customer effort, vulnerable areas ( $A_v$ s) for mobility, firepower, and catastrophic kills resulting from steel and tungsten fragments impacts were calculated. A Vulnerability Analysis of Surface Targets (VAST) (Nail 1982) study of the same missile launcher was subsequently performed to evaluate the differences between COVART III and VAST predictions. View-averaged  $A_v$ s were calculated and compared across a spectrum of fragment impacts: 1 to 5,000 grain steel fragments and 5 and 8 grain tungsten fragments with striking velocities of 500 to 10,000 fps. The differences that were found to occur as a result of this initial comparison stimulated interest in a more extensive model comparison effort. These comparisons are the subject of this report.

1.1 Objective. The objective of this effort was to compare COVART III and VAST for the purpose of developing a more detailed understanding of their differences and similarities. Quantitative comparisons were made with the objective of identifying the cause of differences. Subjective comparisons on ease of code use and usefulness of documentation were also made.

1.2 Approach. The initial  $A_v$  comparison was made using the same target description and criticality analysis. Since the form of input for component probability of kill given a hit ( $P_{k/h}$ ) functions differ between the codes, it was necessary to approximate the functions used in COVART III for input to VAST. Various other input differences were noted in the initial  $A_v$  comparison. These differences were removed for subsequent cell-by-cell probability of kill ( $P_k$ ) comparisons. Histograms were made to compare the distribution of  $P_k$  results for each view. Averaged  $P_k$  for each view were also compared.

Because VAST and COVART III are both deterministic models, differences in results cannot be attributed to random variability and any difference must therefore be considered statistically significant. For this comparison, the judgment of practical significance is probably of more importance than that of statistical significance.

VAST and COVART III cell-by-cell predictions of mobility, firepower, and catastrophic kill probabilities were compared for the following subset of fragment masses and velocities listed previously:

(a) 5, 30, 120, and 700 grain steel fragments at velocities of 2,000 and 5,000 fps, and (b) 5 and 8 grain tungsten fragments at velocities of 2,000 and 5,000 fps. Azimuth and elevation combinations of (90, 0), (90, 45), and (90, 90) degrees were evaluated for both steel and tungsten fragments.

Finally, because differences in cell-by-cell  $P_k$  predictions were noted, calculations for one shotline and one steel fragment were tracked through each code to identify specific differences in the penetration equations used for steel fragments.

## 2. EXPERIMENTAL SETUP

This section presents the comparative information in six basic areas:

- (1) General observations
- (2) View-averaged  $A_v$ s
- (3) Cell-by-cell  $P_k$  differences
- (4)  $P_k$  histograms
- (5)  $P_k$  averages
- (6) Penetration algorithms.

General observations concerning differences in the two codes have been presented first. Some basic differences in code inputs were found to exist in the view-averaged  $A_v$  comparison. These differences, which occurred as a result of the distinct techniques employed to develop inputs for each code, are noted in section 2.1., General Observations. An attempt was made to standardize inputs for the cell-by-cell comparison, histogram, and average  $P_k$  comparisons.

2.1 General Observations. Figures 1 and 2 present an overview of the processes required for the completion of analytical efforts using the VAST and COVART III codes, respectively. Some basic differences in approach can be observed by comparing these two flow charts. Both analysis procedures begin with the U.S. Army Ballistic Research Laboratory Computer-Aided Design (BRL-CAD) target description, which was used to generate the shotline data used by both codes.

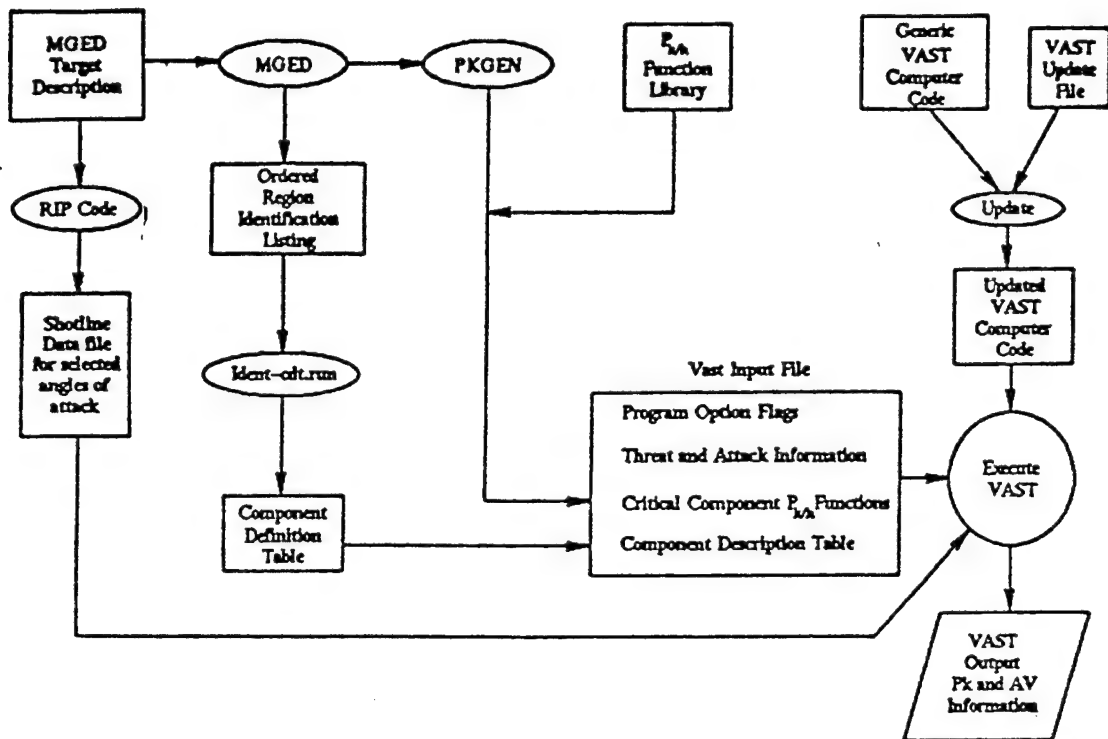


Figure 1. Flow chart of a VAST kinetic energy (KE) fragment analysis process.

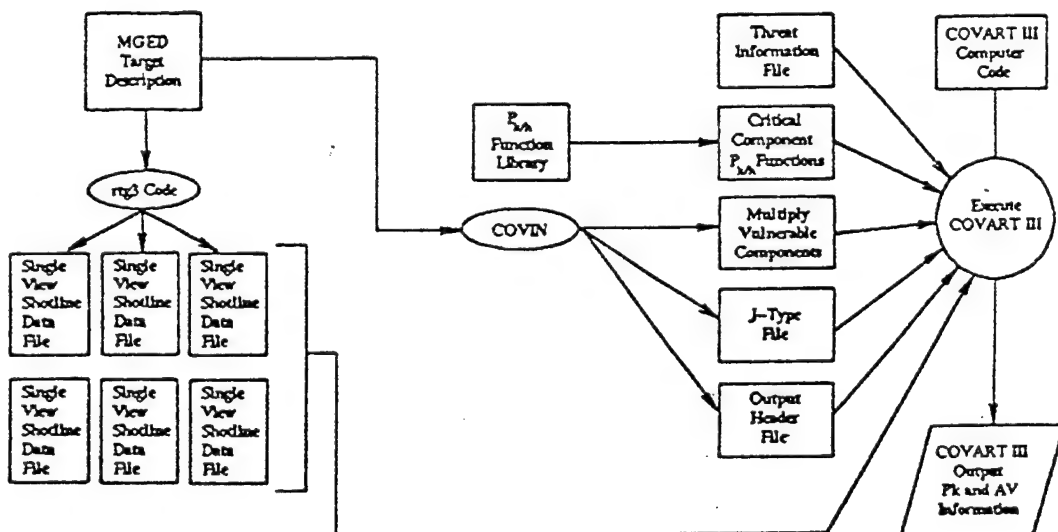


Figure 2. Flow chart of a COVART III KE fragment analysis process.

2.1.1 Ray-Tracing (Shotline) Techniques. First, although each code uses an MGED target description, VAST users within the Logistical and Tactical Targets Branch (LTTB) typically use the Rays Initiated at a Point (RIP) code, and COVART III users in the Air Systems Branch (ASB) typically use the rtg3 code to ray trace the target. The RIP program is used to generate one shotline file containing all of the different views, while the rtg3 program is used to generate shotline data per view. Shotline data are stored in separate files for each view due to computer constraints; however, this enables the COVART analyst to interrupt an analysis, store the intermediate results, and continue the analysis at a later time.

While both the RIP and rtg3 ray-tracing techniques can be utilized to select center cell or random position shotlines, neither code creates input that is compatible with both VAST and COVART III.

For the purpose of comparing the codes, differences resulting from the shotlining techniques were avoided through the use of the Geometric Information For Targets (GIFT) ray-tracing routine, which was able to produce both VAST and COVART III compatible output. Instead of selecting the location of the shotline randomly within each grid, the center of the grid was selected.

2.1.2 Generating Inputs. VAST users utilize the "idents" command within MGED to generate a region component listing, which is then reformatted into the Component Definition Table (CDT) format. The CDT contains all material-type information for all regions as well as the line-of-sight multiplier,  $P_{k/h}$  location and vulnerable category information (if the component is critical), and the region identification number. This is then incorporated into the VAST input file with the  $P_{k/h}$  function information, program option flags, and threat information.

An input-generating code called COVART INput (COVIN) is used to generate input files for COVART III. COVIN uses the MGED target description and user-supplied information to generate a separate file for each type of input: the threat information file, the multiply vulnerable components file, the J-type file, and the output header file. The multiply vulnerable components file describes component relationships in a manner similar to the Standard Damage Assessment List (SDAL) used in VAST. It maps components together in series or parallel relationships needed to assess a function kill. The J-type file is similar to VAST's CDT. It contains material information along with component  $P_{k/h}$  mapping. In addition, the COVART analyst must build a file containing the threat and attack information. Once these files are assembled and properly formatted, the COVART analyst can run COVART III.

Once the VAST input file containing program option flags, threat and attack information, and critical component  $P_{k/h}$  functions and the component description table is generated, the analyst creates a VAST update file that contains any additions or alterations to the original VAST code. The VAST update file and the original VAST code are combined to create an updated version of VAST. This analysis-specific version of VAST is then run using the VAST input file and the shotline data file as inputs. Code updates are not typically made by the COVART analyst.

**2.1.3  $P_{k/h}$  Functions.** In VAST, two- or four-step functions are typically used to provide the  $P_{k/h}$  by a fragment of specified weight and velocity. COVART III uses a piecewise linear function or an exponential function.

The  $P_{k/h}$  functions used in VAST are either obtained from a library of previously generated  $P_{k/h}$  functions or generated using the Probability of Kill Generator (PKGGEN) program. The  $P_{k/h}$  functions used in COVART III are obtained from a library of existing  $P_{k/h}$  functions or by building a new  $P_{k/h}$  function. The piecewise linear functions that were used in the initial COVART III analysis were approximated using step functions as input to VAST for the purpose of these comparisons.

**2.1.4 Kill Definitions.** COVART III analyses of aircraft vulnerability typically use a larger set of kill definitions than are used for ground systems with VAST. While it is possible to address mobility, firepower, and catastrophic kills, the COVART analyst typically analyzes attrition, forced landing, and mission abort for rotary wing aircraft, and catastrophic, a kill <30 seconds, a kill <5 minutes, and a kill <30 minutes for fixed wing aircraft. Definition of kill types is an input difference rather than a coding difference and was not an issue in the quantitative comparisons performed for this effort.

**2.1.5 Personnel Incapacitation.** Crew kill and incapacitation are handled differently in VAST and COVART III. Because of the limited scope of this effort, these differences were not evaluated in detail, but were noted to occur as a result of the fact that the codes were developed separately and have significantly different histories. These differences were eliminated for the purpose of cell-by-cell comparisons by excluding personnel as contributors to system capability.

**2.1.6 Special Caveats for Aircraft.** One of the issues raised during the course of this effort was the question of whether or not COVART III had special caveats for aircraft embedded within it that may not be appropriate for ground system analyses. In discussions with analysts familiar with COVART III

(Anderson, Weaver, and Ten Broeck 1993), no such special caveats were identified. However, it was found that COVART III input requires a specification of aircraft altitude that may be set to zero for ground systems as was done for the comparisons in this report. Also, as will be noted in section 2.6, COVART III allows for input of aircraft speed so that fragment velocity can be calculated relative to aircraft velocity.

2.1.7 Behind Armor Debris Modeling Capability. COVART III does not currently have a behind armor debris modeling capability. VAST has a simple spall model for aluminum armor and the ability to accept updated spall models. To use another spall model in VAST, the code must be updated with the new algorithm using the update procedures discussed in section 2.1.2. Spall was not modeled for the purpose of the comparisons.

2.1.8 Repair Time Modeling Capability. COVART III has a capability to perform estimated repair time calculations that VAST does not. Repair time was not a factor in the comparisons made for this study.

2.1.9 Model Input Requirements and Format. The accepted input format differs between VAST and COVART III. While each style of format entry has its own advantages, the VAST input procedure is a more straightforward, concise method for inputting the required data, making it much easier to assemble and edit the data in the input file. Overall the VAST analysis is easier to manage since there are fewer input and output files required.

2.1.10 Documentation. The documents available on both codes were a bit cryptic in places and have not been updated to reflect changes in terminology or methodology. The available VAST documentation is easier to comprehend than that which is currently available for COVART III. A new COVART III user's manual is under development; however, this document has not been reviewed.

2.2  $A_v$  Comparisons. Figure 3 is a plot of  $A_v$ s for a mobility kill over a spectrum of steel fragment weights and velocities as found using VAST. Figure 4 is a plot of  $A_v$ s for the same steel fragment weights and velocities (but also including some tungsten results) as found using COVART III. Similar plots were also made for mobility and catastrophic kills. Although the trends look basically the same, COVART III results for steel fragments tended to be higher, which is most observable at the high and low ends of the velocity spectrum.

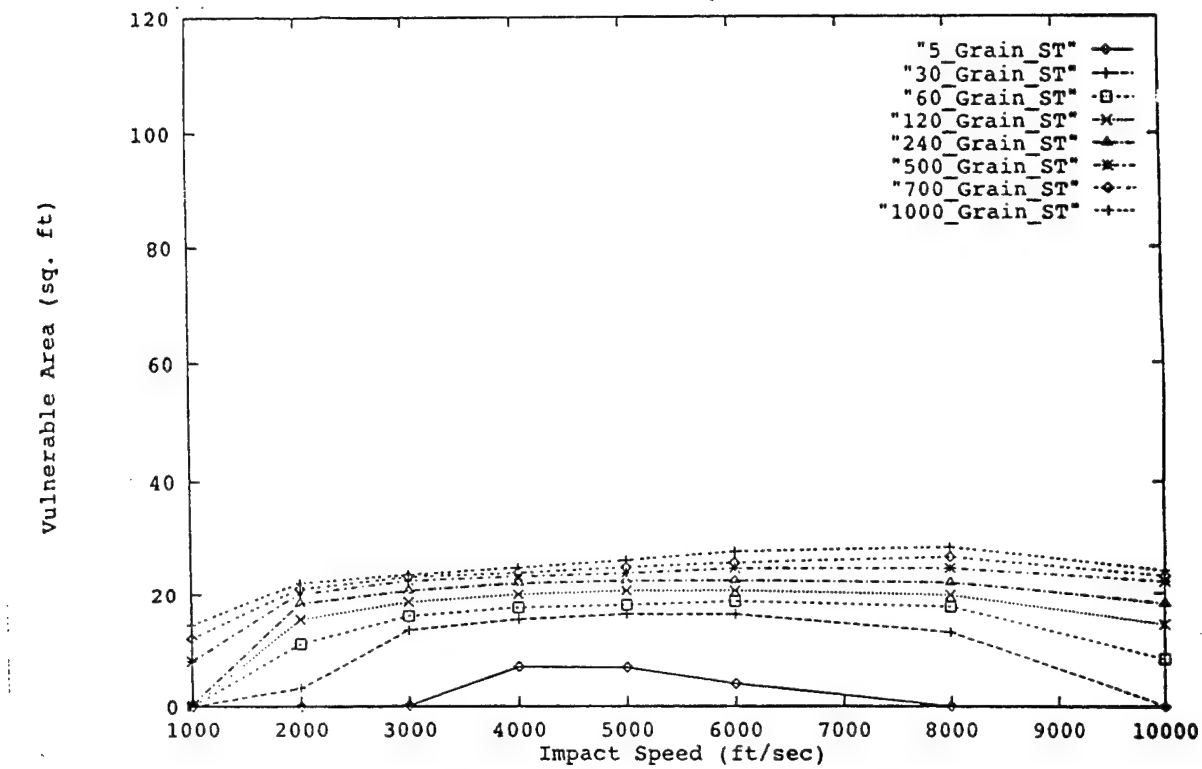


Figure 3. Plot of  $A_v$ s calculated using VAST for a mobility kill.

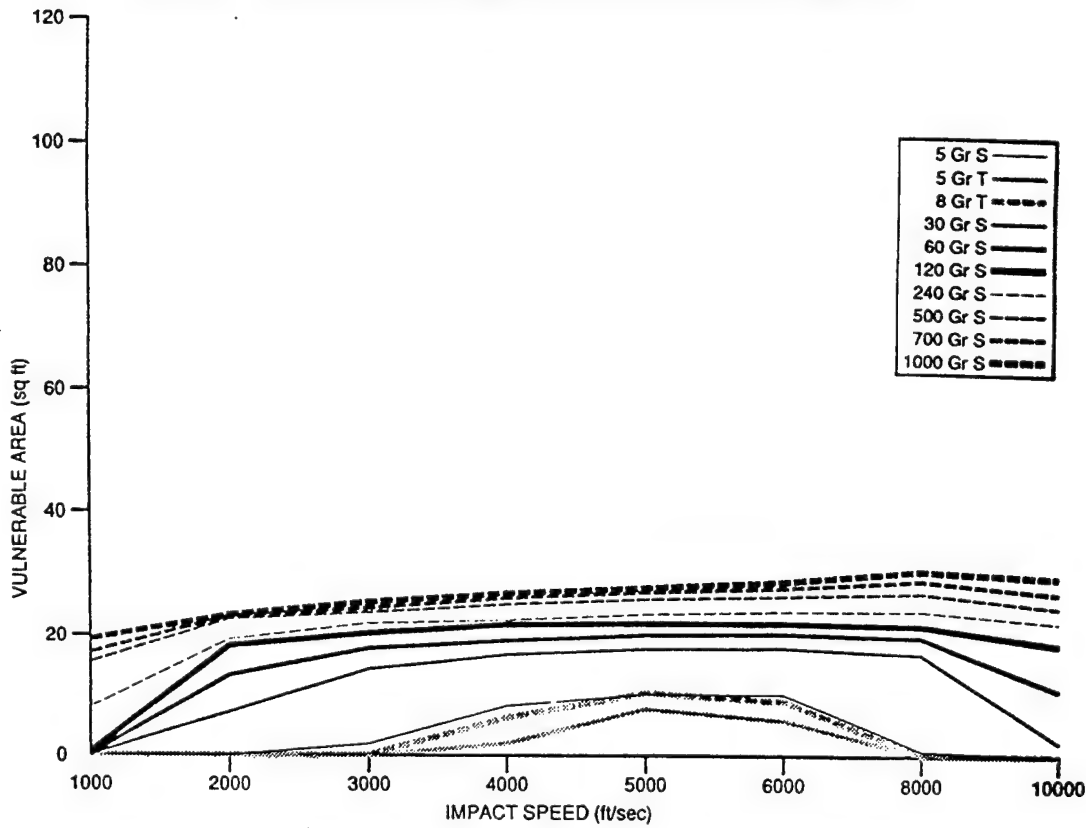


Figure 4. Plot of  $A_v$ s calculated using COVART III for a mobility kill.

It was determined that differences existed in the shotline files and  $P_{k/h}$  functions modeling personnel incapacitations that were used to generate these data. These differences were removed, as described in section 2.1 of this report, to standardize inputs. Once inputs were standardized, model results were compared again, but instead of comparing view-averaged  $A_v$ s, differences in cell-by-cell  $P_k$ s were examined.

**2.3 Cell-by-Cell  $P_k$  Differences.** The differences in the cell-by-cell  $P_k$  assessments made by each code were calculated and plotted for specific views and weight-velocity combinations for steel and tungsten fragments. The  $P_k$ s were assessed for 4-inch grid cells. COVART III outputs the cell-by-cell  $P_k$  assessment to one significant digit. For this comparison, VAST  $P_k$ s, which are usually output with three significant digits, were also rounded to one significant digit using the same algorithm used in COVART III:

$$P_k = \left( \frac{1}{10} \right) \text{INT} (10 \times (P_k) + 0.5) .$$

The cell-by-cell difference plots for a set of steel fragment comparisons were made, although they are not presented here. These plots showed that given equivalent targets (shotline input, critical component definitions, and kill criteria), VAST and COVART III produced different results across 4-inch grid cells for most of the cases analyzed. Since the codes produced different results for the same shotline, histograms were made to determine whether the distribution of  $P_k$ s across each view were also different.

**2.4 Distribution of  $P_k$ s by View.** The distribution of  $P_k$ s for each view was compared by plotting a histogram like those shown in Figures 5 and 6. The  $P_k$  bins were chosen on the basis of the  $P_k$  output provided by COVART III. Bin values can be interpreted as the number of cells for which reported  $P_k$ s were within the following ranges: zero to  $<0.05$ ,  $0.05$  to  $<0.15$ ,  $0.15$  to  $<0.25$ , and so on. Appendix A contains a sample of these histograms for which distributions were found to be different.

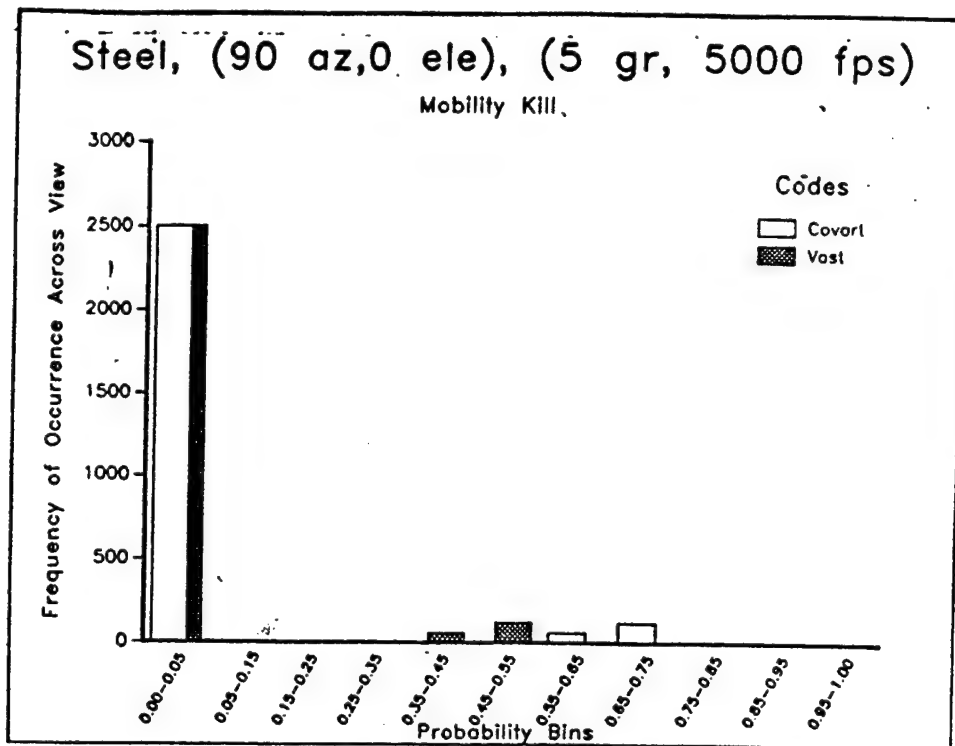


Figure 5.  $P_k$  histogram for a mobility kill given 5 grain, 5,000 fps steel fragment impact at 90° azimuth, 0° elevation.

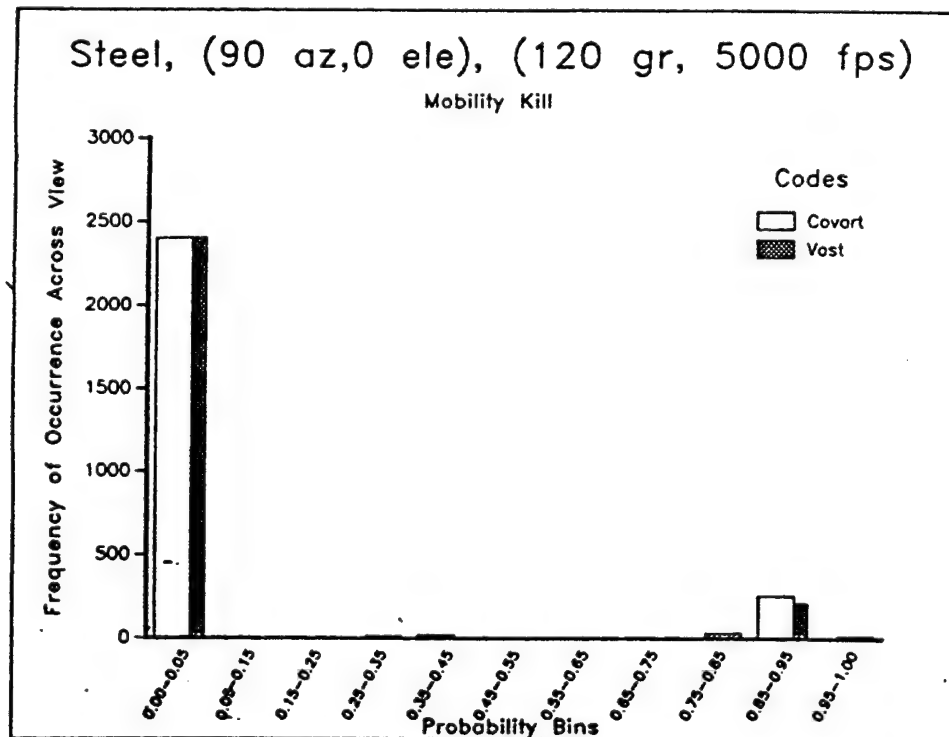


Figure 6.  $P_k$  histogram for a mobility kill given 120 grain, 5,000 fps steel fragment impact at 90° azimuth, 0° elevation.

The following trends were noted:

- distributions of VAST and COVART III firepower kill probabilities were identical across both steel and tungsten data sets.
- distributions of VAST and COVART III mobility kill probabilities were the same for the following sets of conditions:
  - (1) the 5 grain, 2,000 fps steel fragment at the (90, 45) and (90, 0) view angles
  - (2) the 700 grain, 2,000 fps steel fragment at the (90, 45) and (90, 0) view angles
- distributions of VAST and COVART III catastrophic kill probabilities were the same as those observed for mobility kill probabilities.

Distributions of VAST and COVART III mobility (and catastrophic) kill probabilities for the steel fragment cases not listed in (1) and (2) were different. There were some cases in which the distributions were similar (heights and number of bins were the same), but for which the COVART III predictions were shifted to the right by one or two bins, such as the case shown in Figure 5.

In general, VAST and COVART III tungsten comparisons showed fewer similarities than were observed in the steel fragment comparisons. Typically, VAST predicted higher  $P_k$ s than did COVART III for tungsten fragments. For example, for tungsten fragments traveling at 2,000 fps, COVART III predicted no probability of mobility or catastrophic kills, while VAST assessed kill probabilities above 0.65 across at least 5% of the target view. These differences can be attributed to the use of different penetration equations for tungsten fragments used by the two codes.

**2.5 Average  $P_k$ s by View.**  $P_k$ s were averaged for each view for both the steel and tungsten fragments and are reported in Appendix B (VAST  $P_k$ s were not rounded before averaging for this purpose). For steel fragments, most of the COVART III  $P_k$  averages were either equal to (35 out of the 72 cases) or only one percentage higher than (29 out of 72 cases) VAST  $P_k$  averages. In 4 out of the 72 cases compared, COVART III averages were 3 percentage points higher than VAST averages and in 1 case, the COVART III average was 4 percentage points higher. For tungsten fragments, in 24 out of 36 cases, VAST  $P_k$  averages were either equal to 1 or 2 percentage points higher than COVART III  $P_k$  averages. In 12 cases, however, VAST predicted an average  $P_k$  between 0.05 and 0.07, while COVART III predicted a zero  $P_k$ . These 12 cases were the 5 and 8 grain fragments at 2,000 fps for mobility and catastrophic kills.

**2.6 Comparison of COVART III and VAST Penetration Algorithms.** To account for differences observed in the cell-by-cell  $P_k$  plots, VAST and COVART III algorithms were tracked along one shotline for one steel fragment. It was initially recognized that the two codes use different penetration equations for tungsten fragments, which explained the differences observed in the tungsten results. It was thought that for steel fragments, both codes use modified THOR equations at least over some set of conditions, however, significant differences were found. The following discussion pertaining to COVART III modeling of steel fragments highlights significant differences in the penetration equations used by both codes. The step-through of both the COVART III and VAST steel fragment algorithms for a 120 grain, 5,000 fps steel fragment along one shotline shows how residual weight and velocity assessments for this fragment change following encounters with three critical components. Firepower, mobility, and catastrophic kill assessments along this shotline were also compared.

**2.6.1 COVART III Penetration Algorithms.** The penetration equations found in COVART III are from the latest JTCA/ME (Anti-Air) Penetration "Equations Handbook for Kinetic Energy Penetrators" (1985). Equations for steel fragments were derived from experimental firings with mild steel fragments, the most commonly used warhead material.

Penetration equations are used to describe the relationship between the initial conditions of the impactor and component to the penetrator's final conditions. Equations are expressed using dimensionless parameters in order to make the choice of units for individual calculations unimportant and to facilitate the incorporation of principles of scaling (JTCA/ME [Anti-Air] 1985). The penetration algorithms used within COVART III depend on several initial conditions: fragment speed, size and configuration (shape), and yaw angle, as well as aircraft speed. Input of aircraft speed can be used to calculate the initial fragment speed with respect to the speed of the target component that can create an "effective" initial yaw and fragment speed. Ground systems are assumed to be stationary.

The penetration algorithms used in COVART III also account for fragment-presented area and shape factor after impact. The fragments may undergo "ductile failure" upon impact. Ductile failure is the intense deformation of the fragment upon impact where deformed material is stripped off as perforation proceeds. In COVART III, fragment properties (specifically fragment velocity, size, and shape) change after the perforation of a surface and ductile failure has occurred.

COVART III's penetration algorithms also determine if the fragment will perforate, ricochet, or change its state of motion. The "ballistic limit" ( $V_{50}$ ) within COVART III tests the fragment for the impact velocity required to just perforate the component surface. The  $V_{50}$  depends on the properties of the component and on the fragment obliquity and yaw. The decision between ricochet and perforation is based on a comparison of the impactors velocity with the ballistic velocity limit. If the initial velocity of the fragment exceeds the  $V_{50}$ , then it perforates; if not, then it ricochets. Changes in the impactor's state of motion are calculated differently for fragments, which are determined to pierce, plug, or ricochet. Fragments impacting with significant yaw tend to accelerate a small region of the component and thus push out a portion of the component surface along with the fragment (i.e., a "plug").

COVART III takes into account the fragment failure mode for penetrating and ricocheting fragments to determine for subsequent impacts whether the fragment will be modeled as either an intact projectile, an intact core, or a broken core. The four types of fragment failure are: (1) perforation of the fragment intact, (2) deformation mode of mass loss (fragment does not remain intact), (3) a special deformation-mass loss calculation for steel targets, and (4) shattering of the fragment.

Consider the COVART III penetration algorithm used for the deformation-mode mass loss for steel fragments against steel components. The "critical velocity" ( $V_d$ ), defined by equation 66 in JTCA/ME (Anti-Air) (1985), is evaluated to determine mass (weight) loss. The  $V_d$  for steel fragments impacting steel target material is determined using a special algorithm to determine if the fragment remains intact or if it shatters. Under certain circumstances, steel fragments impacting upon these materials produce no mass loss. If the initial velocity of the fragment is  $< 700 V_d$ , then the fragment remains intact and there is no mass loss modeled; if it is  $> 700 V_d$  but  $\leq 2,500 V_d$ , the special mass loss equation for steel is invoked. For initial velocities  $> 2,500 V_d$ , the modified THOR mass loss equations are invoked.

The following mass loss equation (equation 70) from the JTCA reference is for the case where the steel fragment velocity is  $> 700 V_d$ , but  $\leq 2,500 V_d$ :

$$M_r = M \left[ 1 - 0.1656 \left( \frac{V - V_d}{V_d} \right)^{1.42} \right]$$

where:

$M_t$	= residual weight
$M$	= striking weight (in grains)
0.1656	= deformation mode mass-loss constant for mild homogeneous steel
$V$	= velocity of impactor
$V_d$	= critical velocity of an impactor.

Residual velocity of the fragment is also determined:

$$V_r = \sqrt{(V)^2 - (V_{50})^2} / (1.0 + Q4)$$

where:

$V$	= velocity of impactor
$V_r$	= residual velocity
$V_{50}$	= the ballistic limit for determining perforation of component
$1/(1.0 + Q4)$	= a constant applied when perforation is of the "plugging" mode, equal to 1.0 for the "piercing" mode.

The dimensionless constant, Q4, contains a parameter describing the residual obliquity of the fragment to account for changes in trajectory following perforation. Although the JT/CG/ME methodology contains a variable to allow for changes in residual obliquity of the fragment, a single straight trajectory, as developed through the use of the rtg3 shotline program, is utilized in standard COVART III analyses. In this case, the residual obliquity is set equal to the initial fragment obliquity. The Q4 constant also contains the following parameters accounting for target thickness, the material's specific weight, and the fragment's presented area:

$$Q4 = \left( \frac{\rho A_p T}{(M) \cos \theta} \right)$$

where:

$\rho$	= material specific weight
$A_p$	= presented area of fragment
$M$	= striking weight
$\theta$	= angle of obliquity
$T$	= target thickness

If perforation occurs, the penetrator's weight and velocity are reduced according to the modeling rules implemented in COVART III. If the component is critical, its  $P_{k/h}$  is calculated using impact penetrator conditions by interpolating between the available data points of the piecewise linear component  $P_{k/h}$  curves. The component  $P_k$ s are then combined using the "survivor rule" to determine the shotline  $P_k$  for each kill category.

**2.6.2 VAST Penetration Equations (Steel Fragments).** The penetration equations found in VAST for fragments are from the project THOR (Malick 1963) study. The equations and the appropriate constants were derived from test firings of mild steel fragments into various materials.

Penetration algorithms also exist within VAST for other penetrators such as shape charge jets and bullets. However, these were not a factor in this study.

VAST propagates the penetrator through the target along a shotline. When a component is encountered, VAST checks to see if the component is perforated by calculating the fragment's residual velocity and then compares this to a minimum velocity. If the fragment's residual velocity is less than the minimum velocity, then no perforation occurs. If the fragment's residual velocity is greater than the minimum velocity, then its residual weight is computed. This fragment weight is then compared against a minimum weight. If the fragment weight is greater than the minimum weight, then the component is considered to have been perforated.

If the component is critical, its  $P_{k/h}$  is calculated using the impact conditions of the penetrator. The penetrator continues to propagate on the shotline until total dissipation or all the components on the shotline have been perforated. Once this occurs, all of the  $P_{k/h}$ s are combined using the "survivor rule" to obtain a  $P_k$  for the penetrator along the shotline.

The modified THOR equations used to determine the fragment's residual weight and velocity are:

$$M_r = M_s - 10^{R1} * (SF * T)^{R2} * M_s^{R3} * SEC(A)^{R4} * V_s^{R5}$$

and

$$V_r = V_s - 10^{R6} * (SF * T)^{R7} * M_s^{R8} * SEC(A)^{R9} * V_s^{R10}$$

where:

$M_r$	= residual weight
$M_s$	= striking weight
SF	= fragment shape factor
T	= component thickness
A	= angle of obliquity
$V_r$	= residual velocity
$V_s$	= striking velocity
R(1-10)	= material constants listed in Appendix C.

2.6.3 Evaluation Along a Shotline Using COVART III. The following is a step-by-step walk through of COVART III using a shotline containing the following six components and their corresponding thicknesses for a 120 grain fragment moving with an initial speed of 5,000 fps:

- (1) Missile booster conduit (0.08 in thick)
- (2) Missile booster motorcase (9.08 in thick)
- (3) Missile booster fuel (3.74 in thick)
- (4) Missile booster fuel (3.74 in thick)
- (5) Missile booster motorcase (0.08 in thick)
- (6) Missile booster conduit (0.08 in thick).

The shape factor is a variable that is entered by the analyst in the input package before the run takes place. In this example, the fragment started as a cube.

The first component encountered is component no. 8575, the missile booster conduit. This component consists of mild steel (Brinell Hardness No. [BHN] = 100). The 120 grain steel cube with BHN = 300

strikes the component with a velocity of 5,000 fps. Component no. 8575 is critical for the firepower kill and the resulting  $P_k$ s are:

$$\begin{aligned}P_k \text{ mobility} &= 0.0 \\P_k \text{ firepower} &= 1.0 \\P_k \text{ catastrophic} &= 0.0\end{aligned}$$

These  $P_k$ s were ascertained by the code through the use of a  $P_k$  table based upon the threat's initial weight and velocity and its associated kill level. The fragment's residual weight and velocity, based upon the special penetration equations used for steel in COVART III, as described earlier, are as follows:

$$M_r = 111.97 \text{ grains}$$

and

$$V_r = 3768.28 \text{ fps.}$$

The fragment then engages the next component, component no. 8530, which is the missile booster motorcase made of mild steel. The motorcase is also critical for firepower, and the resulting  $P_k$ s are:

$$\begin{aligned}P_k \text{ mobility} &= 0.0 \\P_k \text{ firepower} &= 1.0 \\P_k \text{ catastrophic} &= 0.0\end{aligned}$$

The penetrator's residual weight and velocity are computed to be:

$$M_r = 110.96 \text{ grains}$$

and

$$V_r = 2,794 \text{ fps.}$$

With its remaining energy, the fragment penetrates the third component on the shotline, component no. 8520, the missile booster fuel. This component is critical to mobility, firepower, and catastrophic kills and produces resulting  $P_k$ s of:

$P_k$ mobility	= 0.9425
$P_k$ firepower	= 0.9425
$P_k$ catastrophic	= 0.9425

The next three components on the shotline are identical to the first three components on the shotline. This is due to the concentric configuration of these components. In COVART III,  $P_k$  calculations are only made once for each component on the shotline.

The grid cell was then evaluated to determine the resulting grid cell  $P_k$ s:

$P_k$ mobility	= 0.9425
$P_k$ firepower	= 1.0
$P_k$ catastrophic	= 0.9425

The code then continues to the next fragment velocity.

**2.6.4 Evaluation Along a Shotline Using VAST.** The following is an example of how VAST calculates the  $P_k$  of a component along the same shotline evaluated using COVART III. For this example, a 120 grain fragment moving with an initial velocity of 5,000 fps and a fragment shape factor of  $0.00875 \text{ in}^2/\text{grain}^{2/3}$  was used.

The process begins with the 120 grain fragment, moving at 5,000 fps, striking the missile booster conduit. The conduit is a critical component for a firepower kill, so the component's  $P_{k/h}$  must be determined. To do this, the program will do a lookup on the component  $P_{k/h}$  function, using the penetrator's initial speed and weight, and determine the appropriate  $P_k$ s:

$P_k$ mobility	= 0.0
$P_k$ firepower	= 1.0
$P_k$ catastrophic	= 0.0

Now VAST computes the fragment's new weight and velocity:

$$M_t = 56.9 \text{ grains}$$

and

$$V_t = 4,145 \text{ fps}$$

The process continues with the 56.9 grain fragment, moving at 4,145 fps, striking the missile booster motorcase. This is a critical component for firepower capability, so the component's  $P_{k/h}$  and then the penetrator's residual weight and velocity are determined. The probability of achieving a kill to this component is:

$$P_k \text{ mobility} = 0.0$$

$$P_k \text{ firepower} = 1.0$$

$$P_k \text{ catastrophic} = 0.0$$

The fragment's residual weight and velocity are:

$$M_t = 29.5 \text{ grains}$$

and

$$V_t = 3,037 \text{ fps}$$

The fragment now encounters the first section of missile booster fuel. The booster fuel is critical for mobility and firepower capability. A penetration into the booster fuel may also result in a catastrophic kill. Using the fragment's initial conditions, the component's  $P_{k/h}$ s are:

$$P_k \text{ mobility} = 0.84875$$

$$P_k \text{ firepower} = 0.84875$$

$$P_k \text{ catastrophic} = 0.84875$$

The fragment does not lose any mass passing through the fuel (liquid), but is slowed to a speed of 1,642 fps. The fragment now encounters the second section of missile booster fuel for which component  $P_{k/h}$ s are determined to be:

$P_k$ mobility	= 0.84875
$P_k$ firepower	= 0.84875
$P_k$ catastrophic	= 0.84875

Again, the fragment does not lose any mass, but is slowed to a speed of 735 fps. The 29.5 grain fragment hits the missile booster motorcase again and produces a  $P_k$  of:

$P_k$ mobility	= 0.0
$P_k$ firepower	= 1.0
$P_k$ catastrophic	= 0.0

The fragment cannot penetrate through the missile booster motorcase, so the shotline is finished. VAST now calculates the total  $P_k$  for  $n = 6$  components along the shotline according to the component kill categories using the "survivor rule":

$$P_{k/h \text{ grid cell}} = [1 - (1 - P_{k/h(1)})(1 - P_{k/h(2)}) \dots (1 - P_{k/h(n)})]$$

$P_k$ mobility	= 0.977
$P_k$ firepower	= 1.0
$P_k$ catastrophic	= 0.977

**2.7 Summary of Differences.** The treatment of fragment failure and the use of the special weight loss equations within COVART III result in differences between COVART III and VAST weight and velocity predictions as demonstrated by the shotline evaluations. The THOR equations are implemented in COVART III when the initial velocity of the impactor is  $> 2,500 V_d$ , the exact value of which depends on  $V_d$ , but which is generally in the high velocity region above 10,000 fps. Since these velocities are not often encountered, differences in model predictions of fragment weight and velocity should be expected more often than not.

Although the form of the THOR equations used in COVART III appear (JTCG/ME [Anti-Air] 1985) different from what is presented elsewhere (Malick 1963), a similar walk-through as presented for the 120 grain, 5,000 fps fragment was performed for a fragment exceeding the 2,500  $V_d$  criteria and it was found that the codes did indeed produce the same weight and velocity.

Another difference was noted in comparing the results of the shotline evaluation when COVART III encountered a symmetrical shotline. VAST evaluated a  $P_k$  for each of the six components along the shotline, while COVART III evaluated only the first three. In fact, there were really only three components that fell along this shotline, but the fragment had to pass into the booster conduit, through the motorcase, into the fuel, and out again. VAST incorporated into the calculation of overall shotline  $P_k$ , the component  $P_{k/h}$ s resulting from the fragment entering and exiting the system, while COVART III considered the fragment entering only.

Differences in model predictions of weight and velocity may not always lead to different kill probabilities, as was evidenced in the comparison of firepower kill along the shotline that was evaluated. This result was due to the nature of the  $P_{k/h}$ s that were used. On the other hand, since the form of the  $P_{k/h}$  functions differed slightly for each code, it is also true that even the same weight and velocity predictions may lead to different  $P_{k/h}$  predictions. The difference in use of penetration equations, however, was the main contributor to differences in model predictions.

### 3. CONCLUDING REMARKS

Although quantitative differences were observed in the cell-by-cell comparisons of steel fragments, these differences do not appear to have practical significance in light of the fact that the typical customer relies on the use of averages and not on the cell-by-cell results for fragmenting munitions. Even though cell-by-cell differences in  $P_k$  assessments were obvious, averages for each view did not differ by more than 3 percentage points for steel fragment comparisons. Differences observed in the  $P_k$ s produced by the tungsten fragments were judged to be significant since in 12 cases, VAST predicted an average  $P_k$  between 0.05 and 0.07, while COVART III predicted a zero  $P_k$  value.

The formulation of the vulnerability/lethality process has been defined within a mathematical framework called the vulnerability/lethality taxonomy or process (Klopcic 1992). Methods such as VAST and COVART III do not adhere to this structure. A number of efforts are underway in the BVLD that will provide a common set of tools or approximation methods to support the performance of vulnerability/lethality analyses according to this taxonomy. The development of the Modular Unix-Based Vulnerability Estimation Suite (MUVES) (Hanes et al. 1991) provides a common operating environment for these approximation methods. The Stochastic Analysis of Fragmenting Effects (SAFE) (Hanes et al. 1991) methods and the Modular Air Systems Vulnerability Network Estimation (MAVEN) will be

implemented under MUVES. Because the MUVES environment is being developed to follow the taxonomy, approximation methods such as SAFE/MAVEN can be applied to the various classes of problems, such as air and light ground systems, that have historically developed similar yet disparate methods.

Various teams within the division have been independently addressing issues that were noted as contributing to disparities found in the VAST and COVART results compared in this report. For example, a process action team (PAT) was established in 1992 to address the vulnerability process step called "Component  $P_{k/h}$ ." The initial efforts of the PAT have been documented (Klopcic 1992). Although not thoroughly investigated for the purpose of this comparison, it was also noted that each code treated the evaluation of personnel incapacitation differently. To some degree, this is a component  $P_{k/h}$  problem and has been addressed by the Component  $P_{k/h}$  PAT. Specific technical efforts are currently ongoing within the BVLD to incorporate the use of the ComputerMan Methodology for the assessment of personnel incapacitation, which will solve this difference.

**INTENTIONALLY LEFT BLANK.**

#### 4. REFERENCES

Anderson, J., E. Weaver, and D. Ten Broeck. Private communication. U.S. Army Research Laboratory, Aberdeen Proving Ground, MD, 1993.

Hanes, P. J., S. L. Henry, G. S. Moss, K. R. Murray, and W. A. Winner. "Modular Unix-Based Vulnerability Estimation Suite (MUVES) Analyst Guide." BRL-MR-3954, U.S. Army Ballistic Research Laboratory, Aberdeen Proving Ground, MD, December 1991.

Joint Technical Coordinating Group for Munitions Effectiveness (Anti-Air). "Penetration Equations Handbook for Kinetic-Energy Penetrators." 61 JTCG/ME-77-16, Aerial Target Vulnerability Subgroup, October 1985.

Klopcic, J. T. "Component  $P_{K/H}$  ( $P_{D/H}$ ,  $P_{I/H}$ ) Exercise." ARL-SR-8, U.S. Army Research Laboratory, Aberdeen Proving Ground, MD, March 1992.

Klopcic, J. T., M. W. Starks, and J. N. Walbert. "A Taxonomy for the Vulnerability/Lethality Analysis Process." BRL-MR-3972, U.S. Army Ballistic Research Laboratory, Aberdeen Proving Ground, MD, May 1992.

Malick, D. "The Resistance of Various Non-Metallic Materials to Penetration by Steel Fragments; Empirical Relationships for Fragment Residual Velocity and Residual Weight." Project THOR TR-51, Ballistic Analysis Laboratory, Institute for Cooperative Research, Baltimore, MD, April 1963.

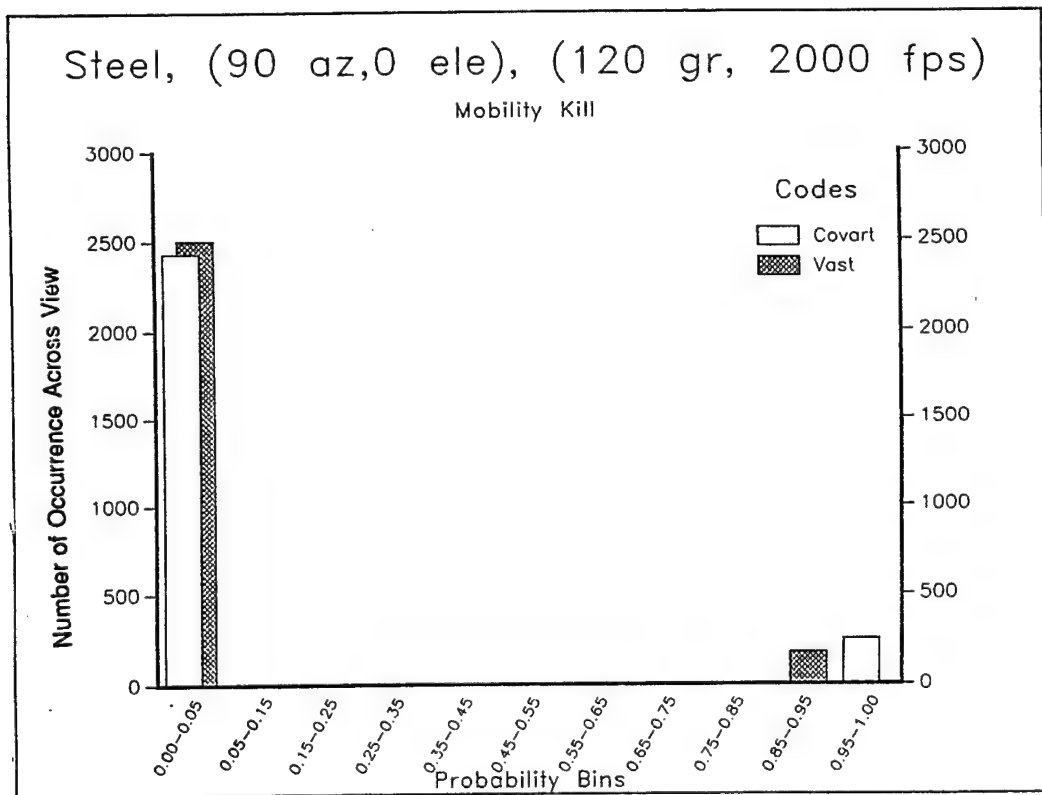
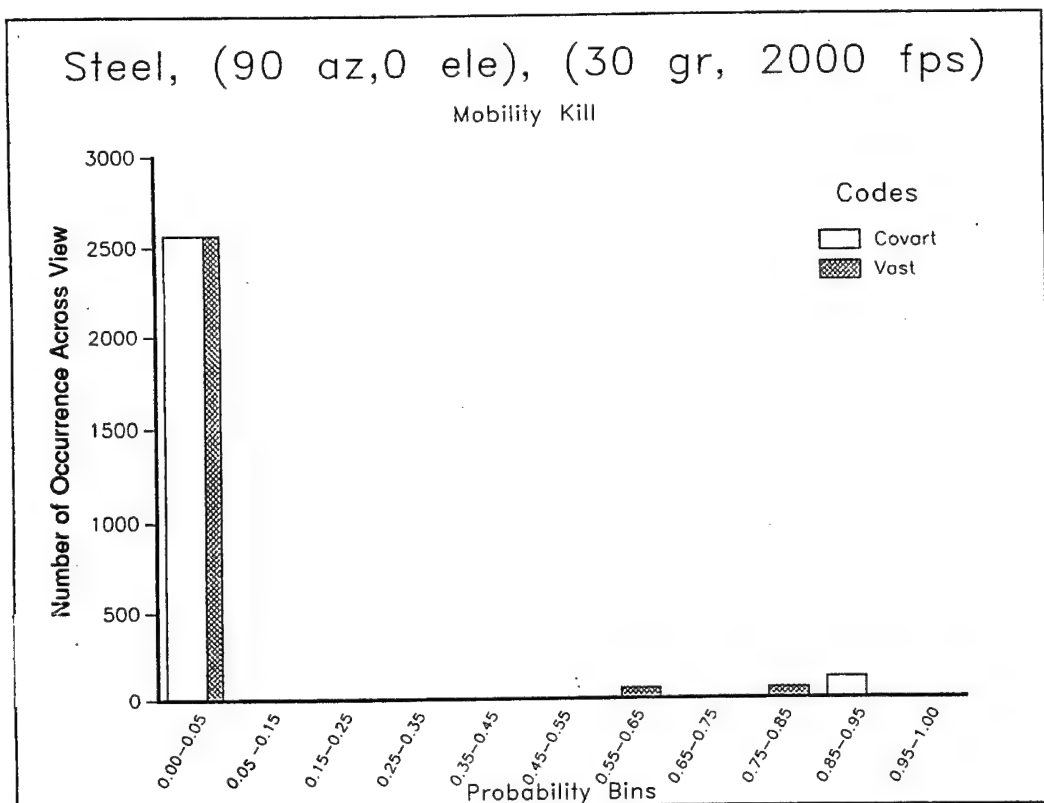
Nail, C. L. "Vulnerability Analysis for Surface Targets (VAST) An Internal Point-Burst Vulnerability Assessment Model-Revision I." CSC TR-82-5740, August 1982.

**INTENTIONALLY LEFT BLANK.**

**APPENDIX A:**  
**HISTOGRAMS**

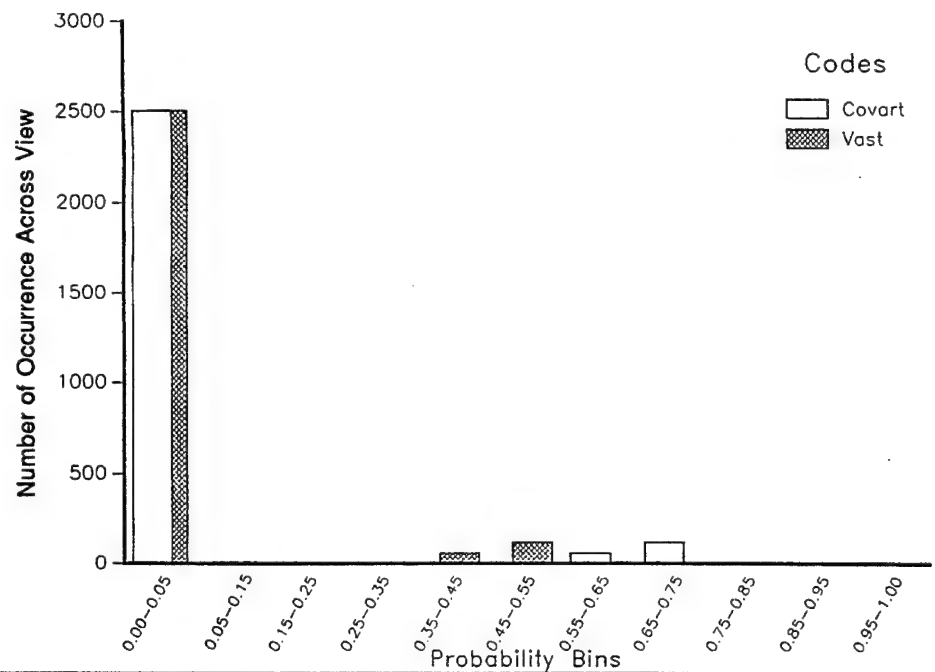
**INTENTIONALLY LEFT BLANK.**

This appendix contains histogram plots of the probability of kill ( $P_k$ ) predictions produced by Computation of Vulnerable Area and Repair Time (COVART III) and Vulnerability Analysis for Surface Targets (VAST) codes for a set of steel and tungsten comparisons for which the distributions of results appeared different. Results for mobility kill category type have been presented.



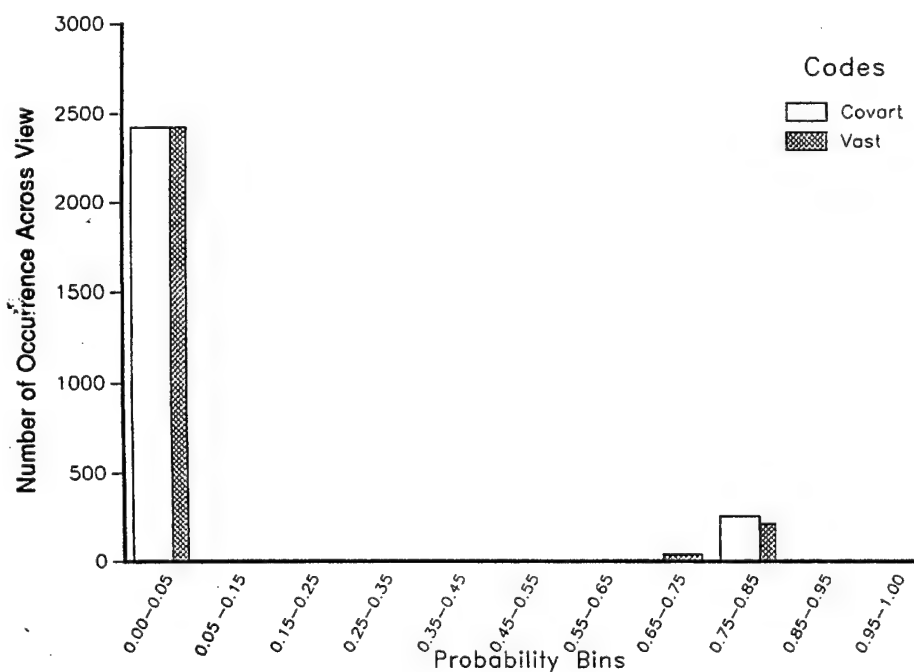
Steel, (90 az,0 ele), (5 gr, 5000 fps)

Mobility Kill



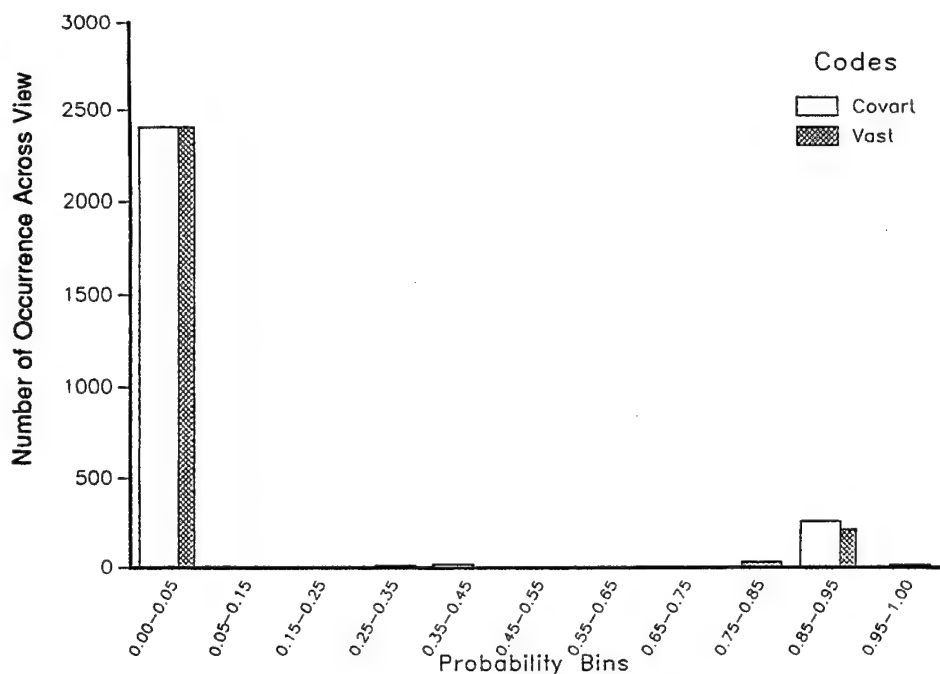
Steel, (90 az,0 ele), (30 gr, 5000 fps)

Mobility Kill



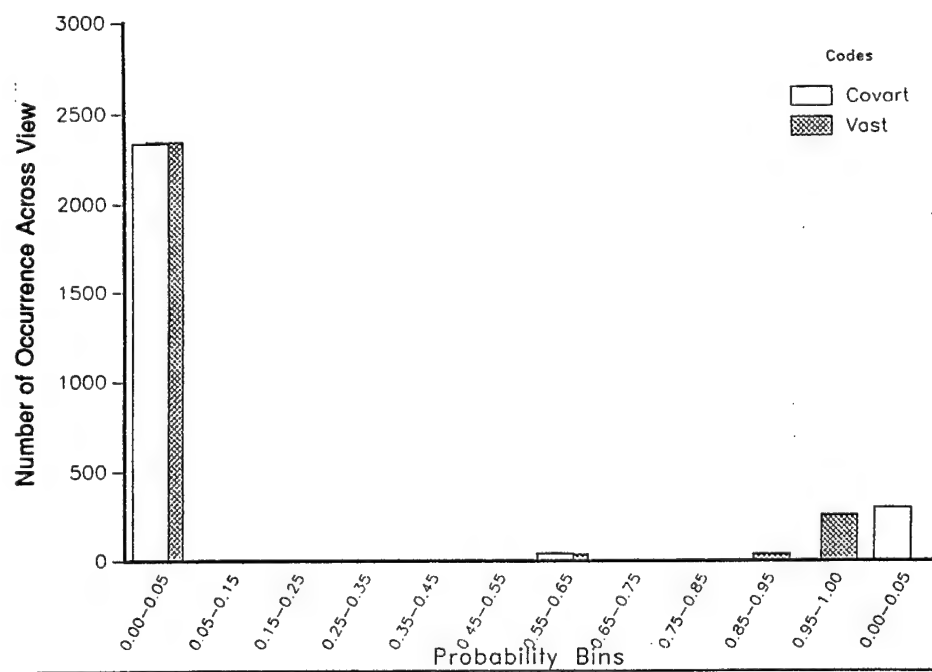
Steel, (90 az,0 ele), (120 gr, 5000 fps)

Mobility Kill



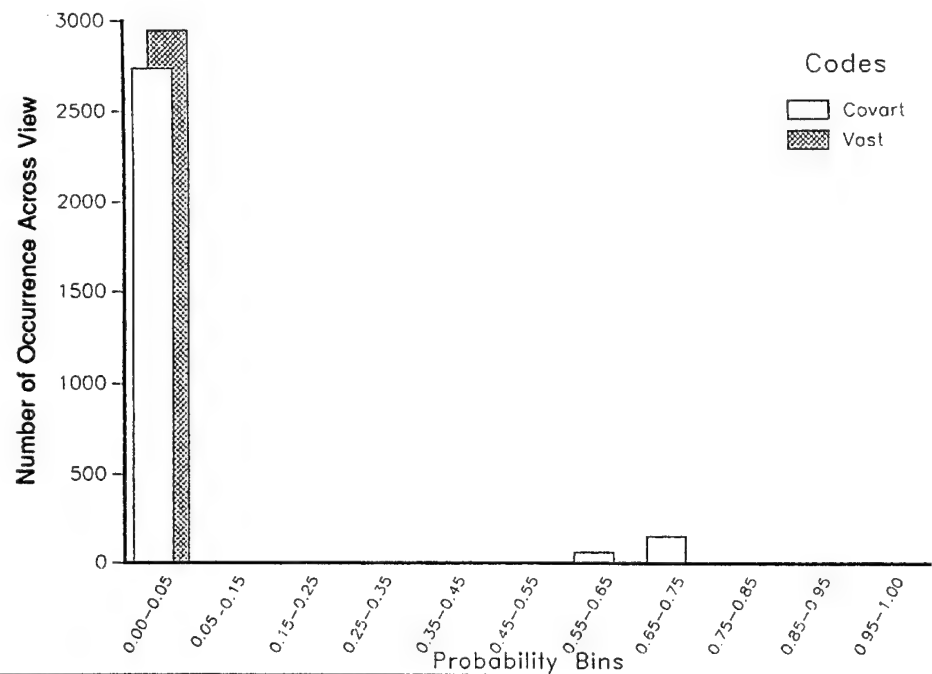
Steel, (90 az,0 ele), (700 gr, 5000 fps)

Mobility Kill



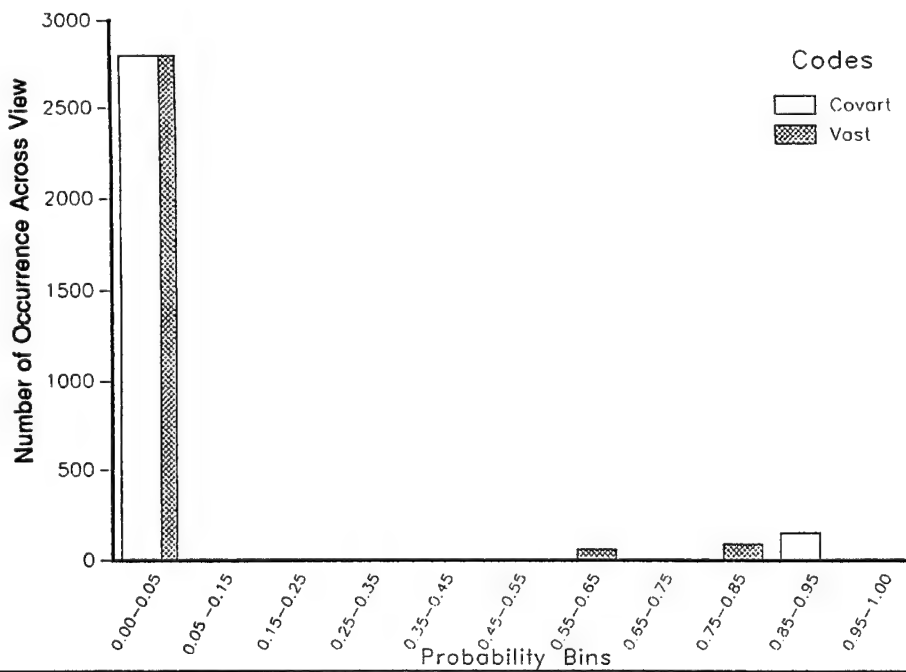
Steel, (90 az,90 ele), (5 gr, 2000 fps)

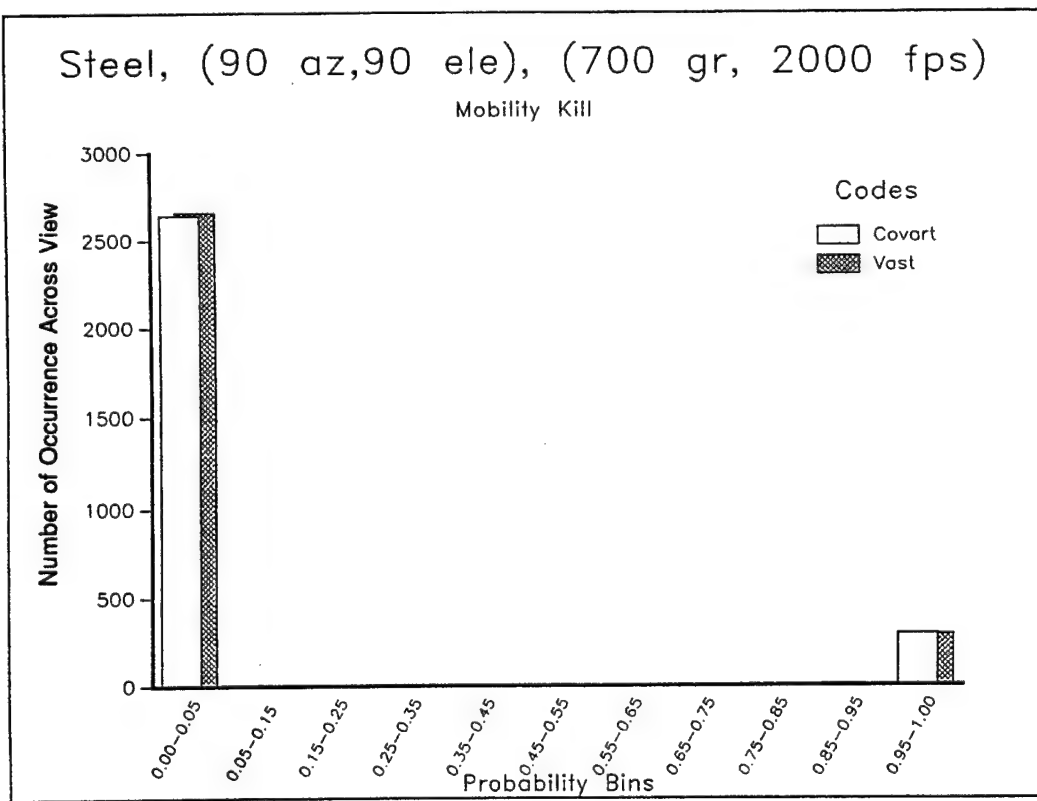
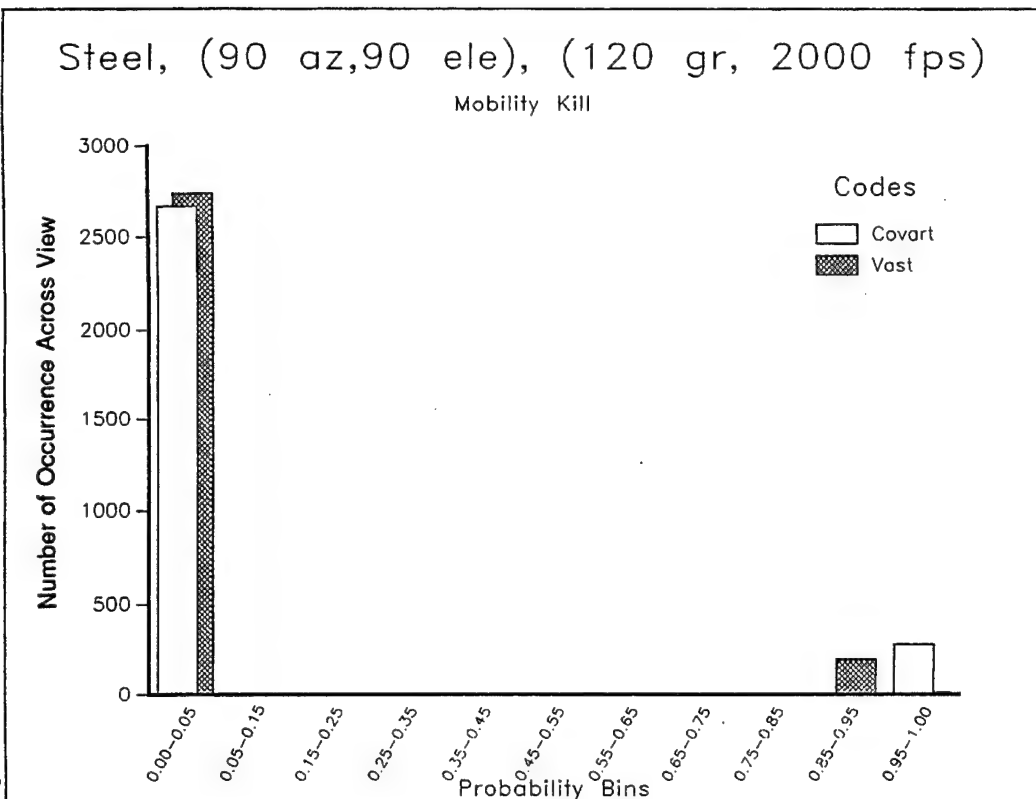
Mobility Kill



Steel, (90 az,90 ele), (30 gr, 2000 fps)

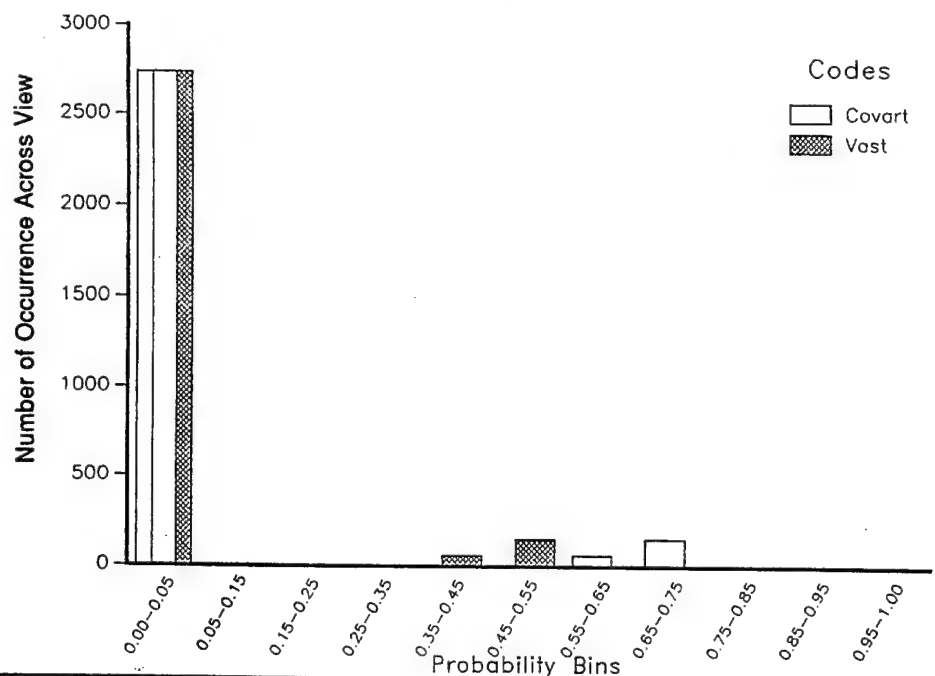
Mobility Kill





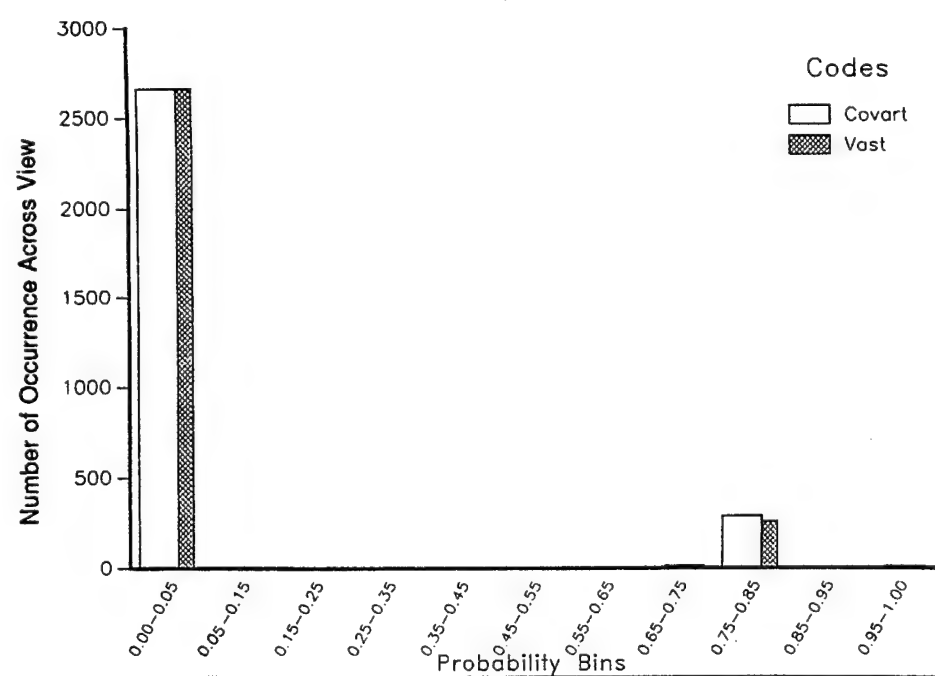
Steel, (90 az,90 ele), (5 gr, 5000 fps)

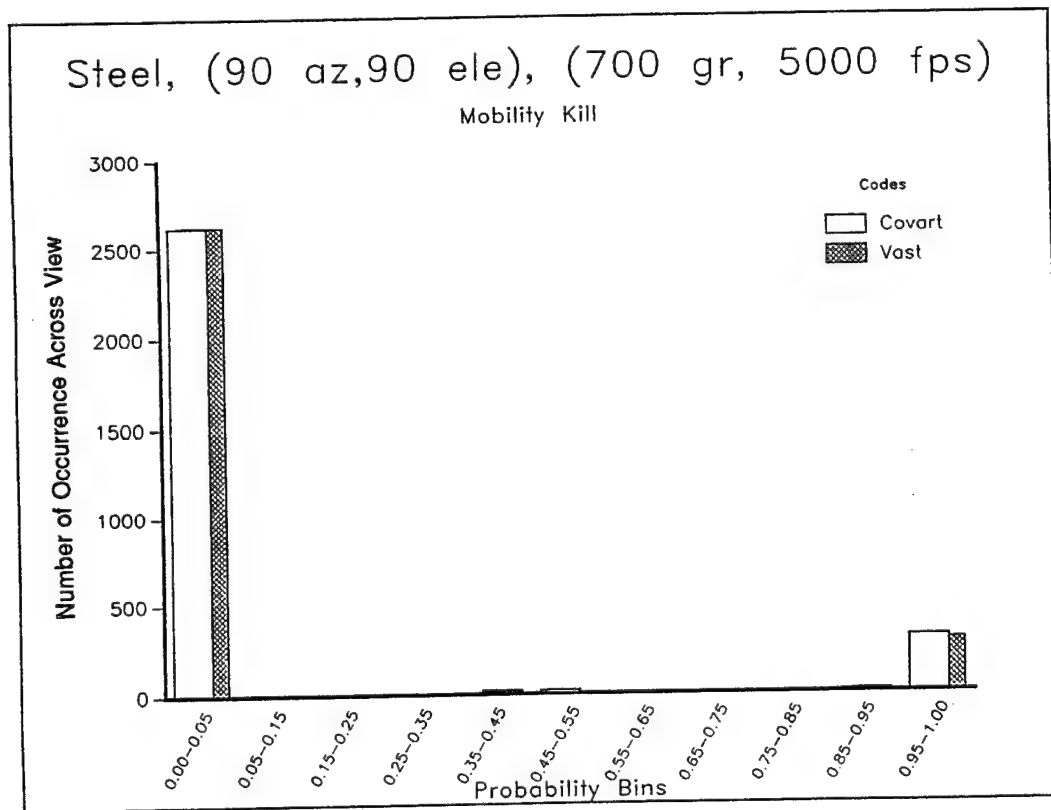
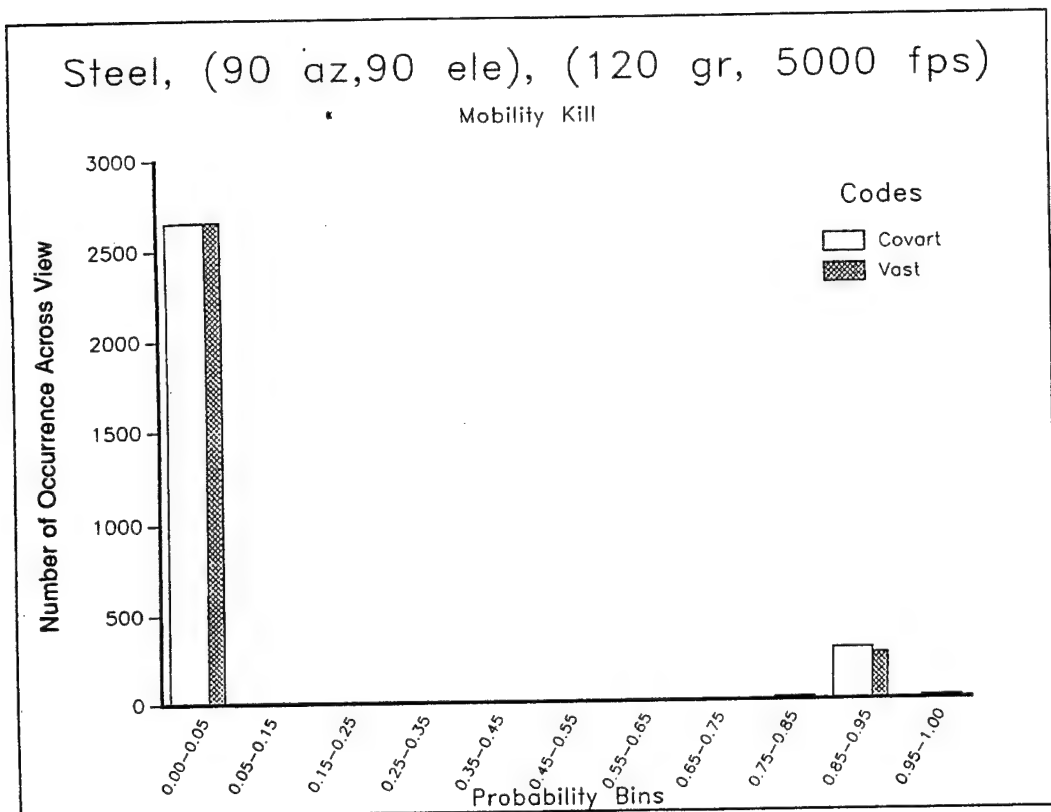
Mobility Kill



Steel, (90 az,90 ele), (30 gr, 5000 fps)

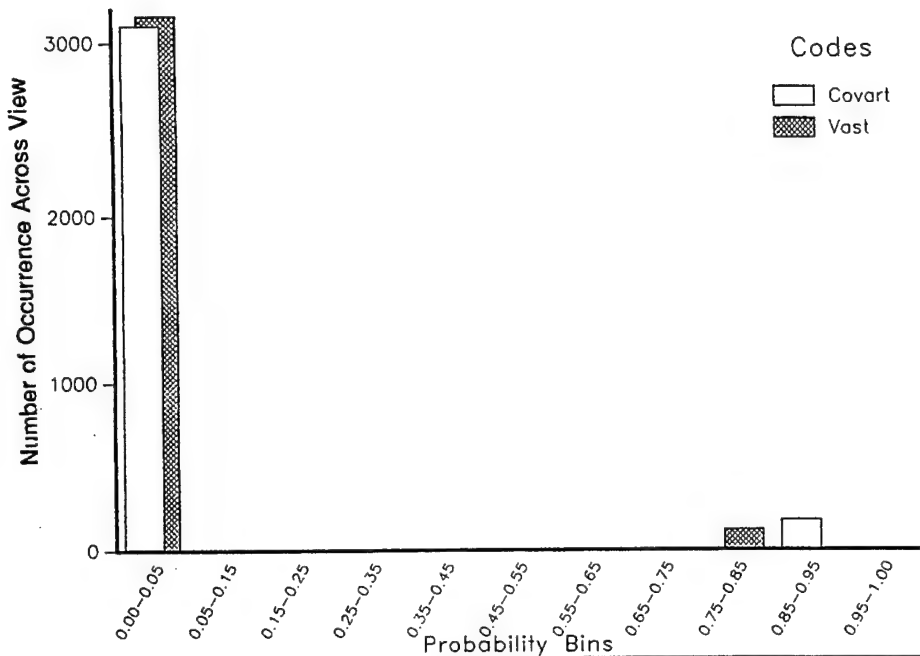
Mobility Kill





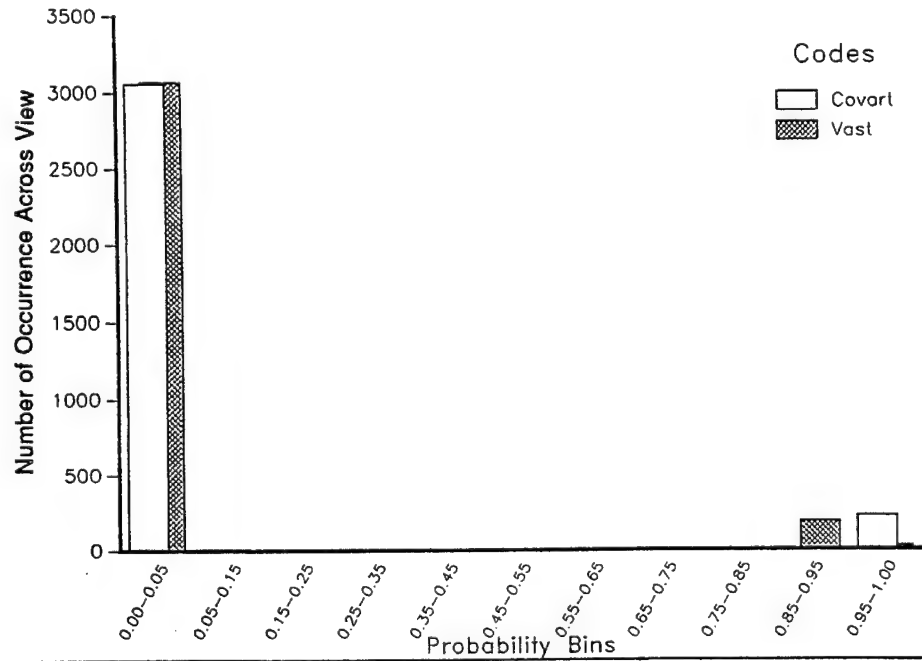
Steel, (90 az,45 ele), (30 gr, 2000 fps)

Mobility Kill

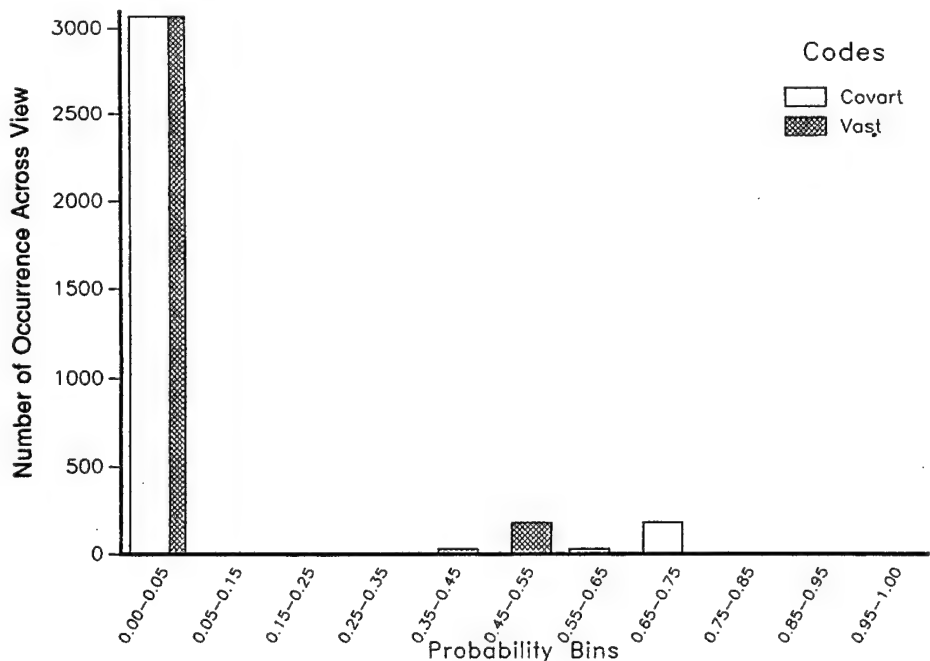


Steel, (90 az,45 ele), (120 gr, 2000 fps)

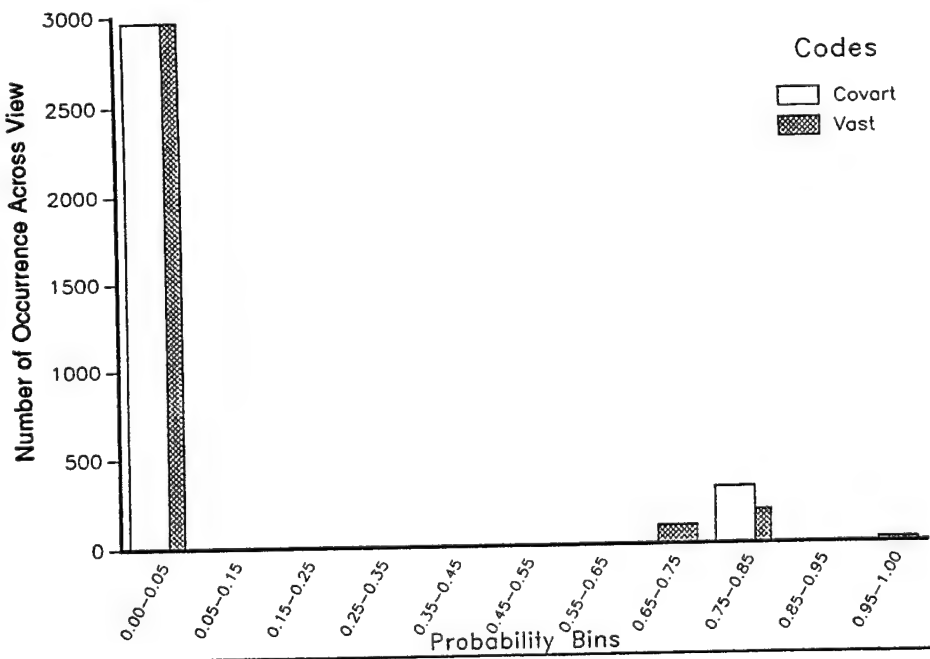
Mobility Kill

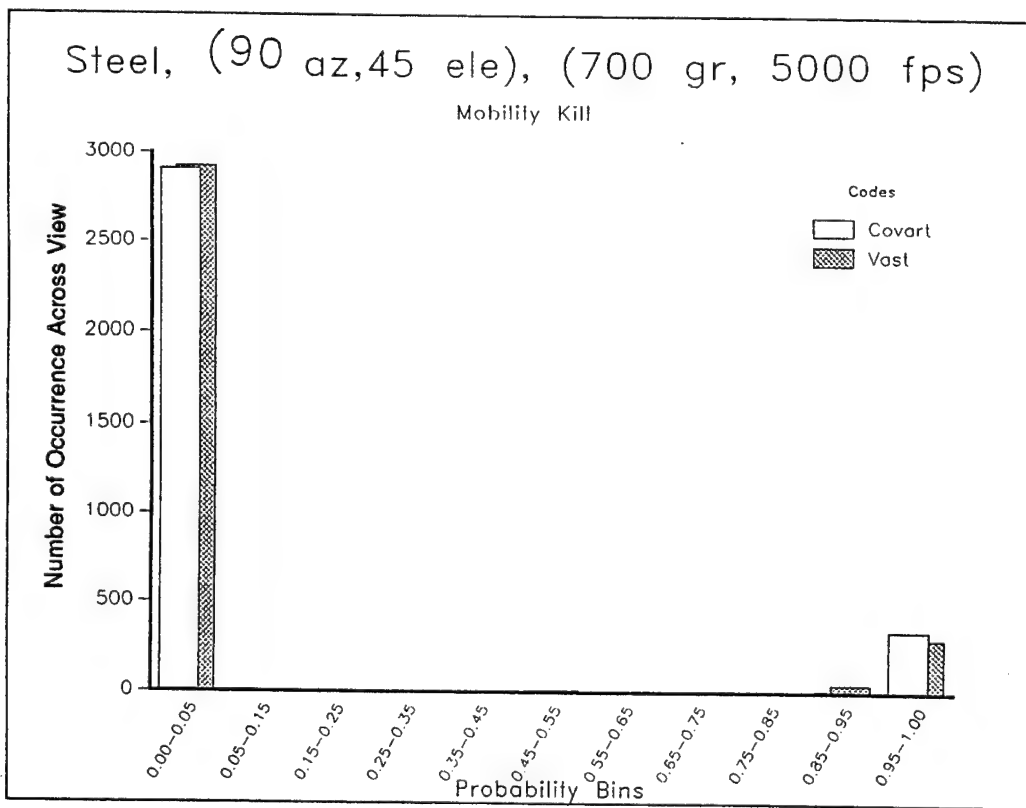
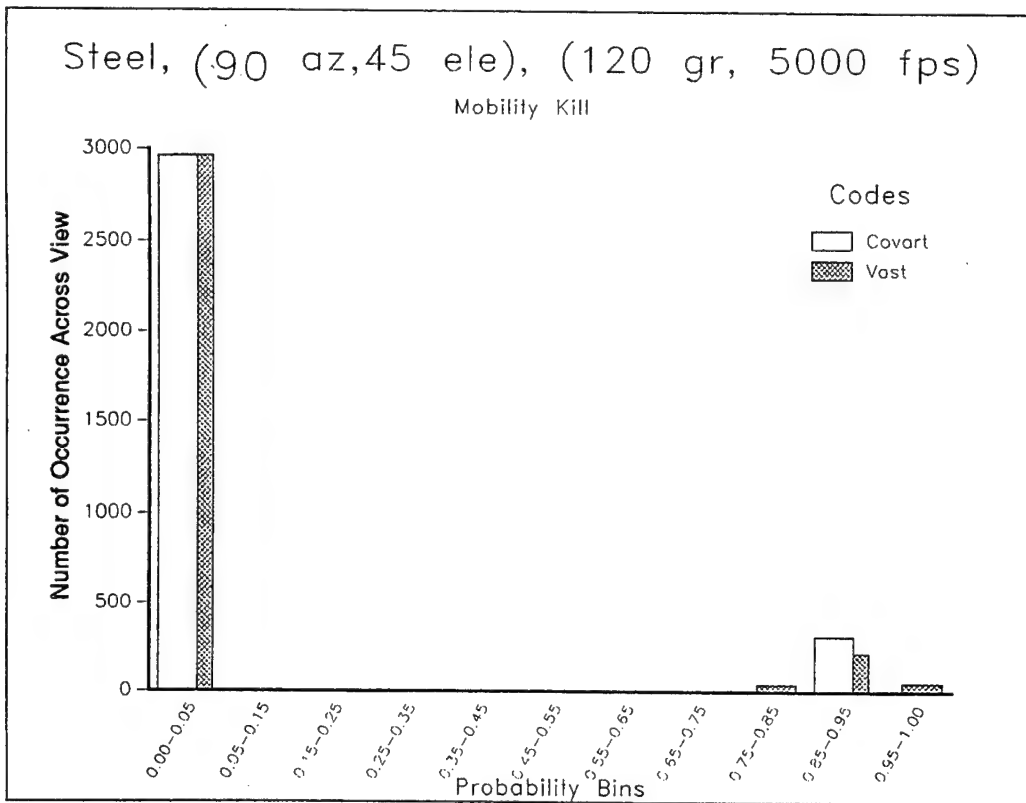


Steel, (90 az, 45 ele), (5 gr, 5000 fps)  
Mobility Kill



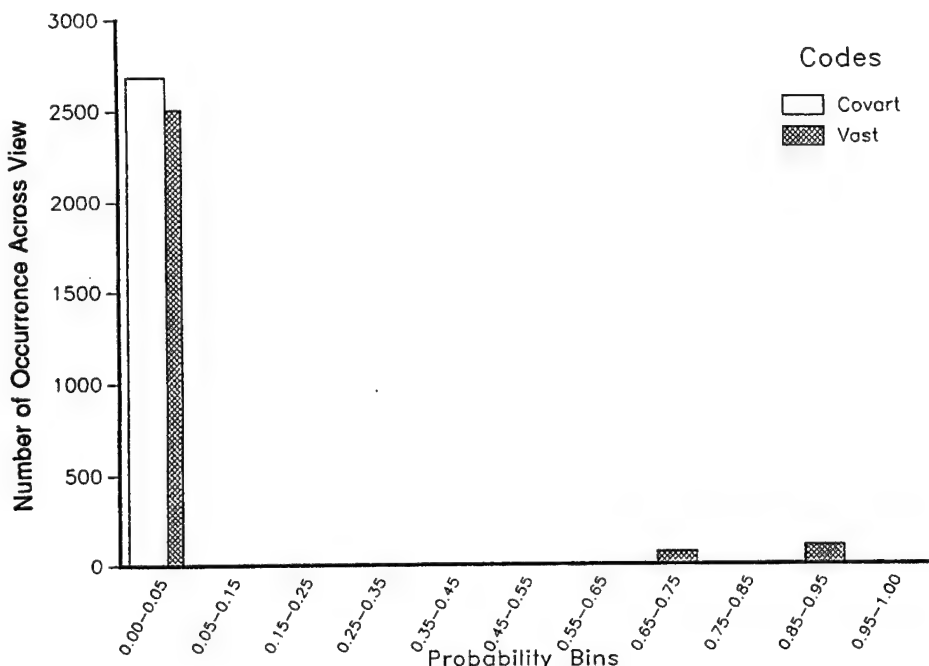
Steel, (90 az, 45 ele), (30 gr, 5000 fps)  
Mobility Kill





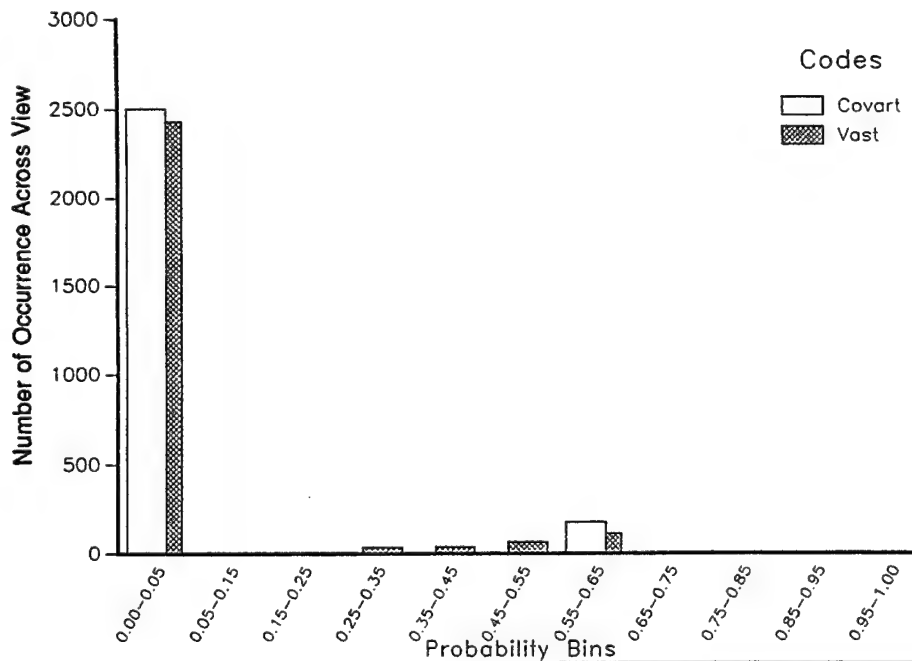
Tungsten, (90 az,0 ele), (5 gr, 2000 fps)

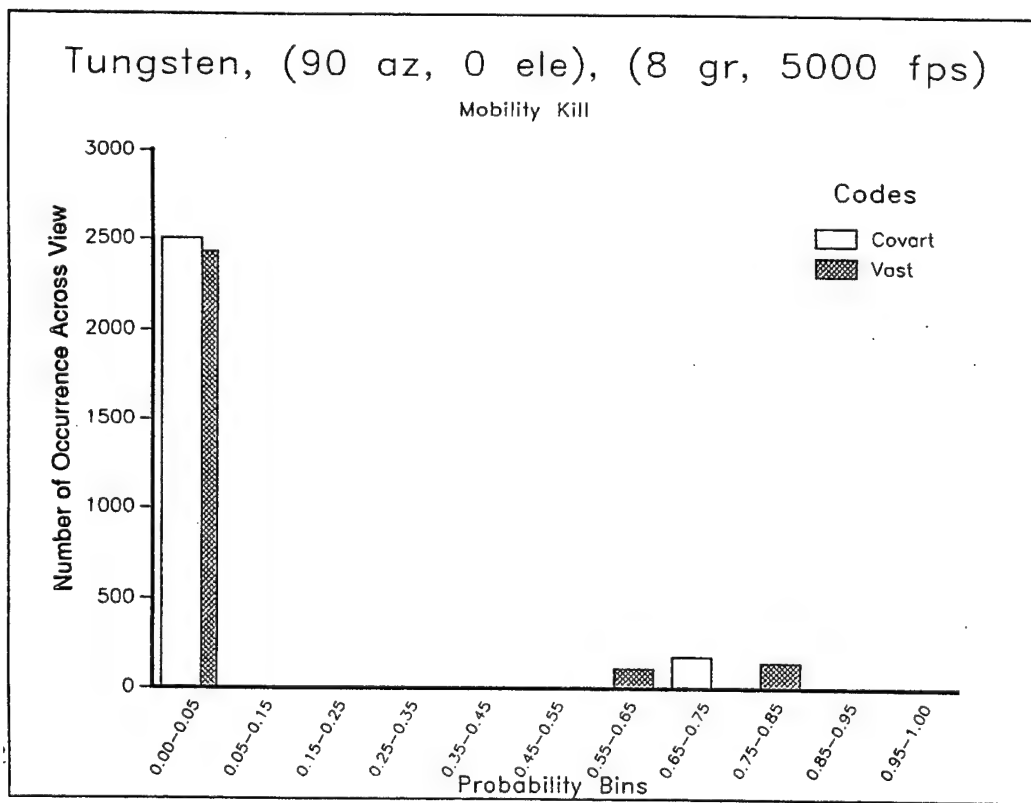
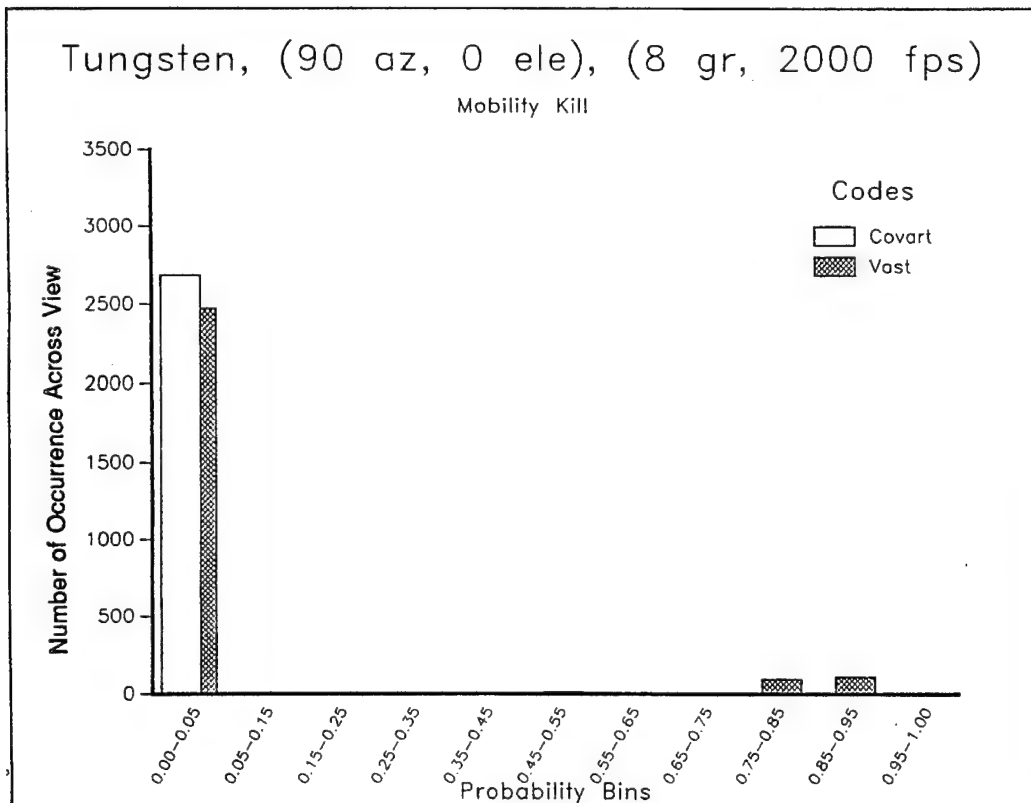
Mobility Kill



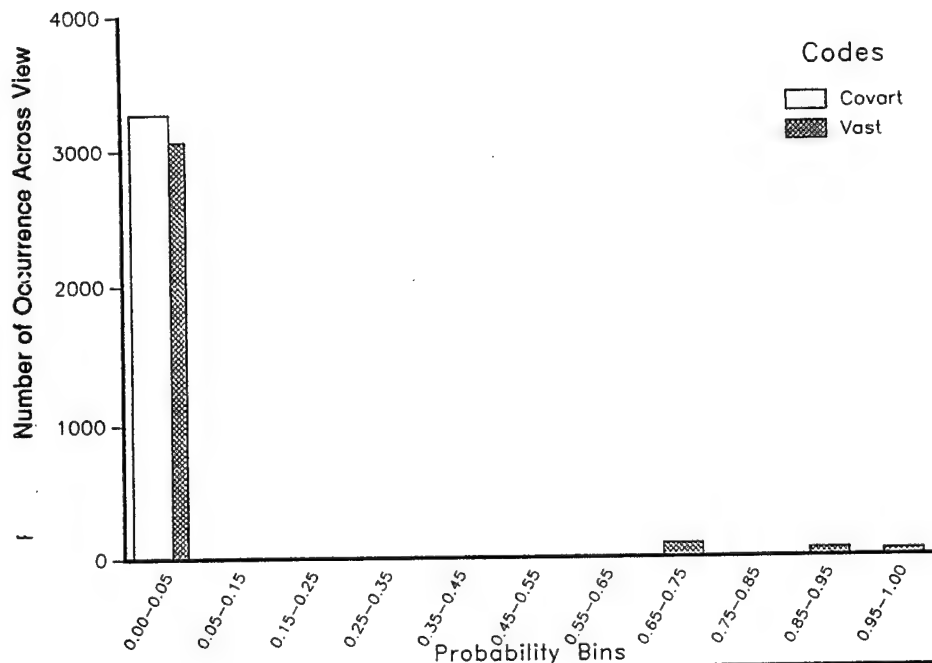
Tungsten, (90 az,0 ele), (5 gr, 5000 fps)

Mobility Kill

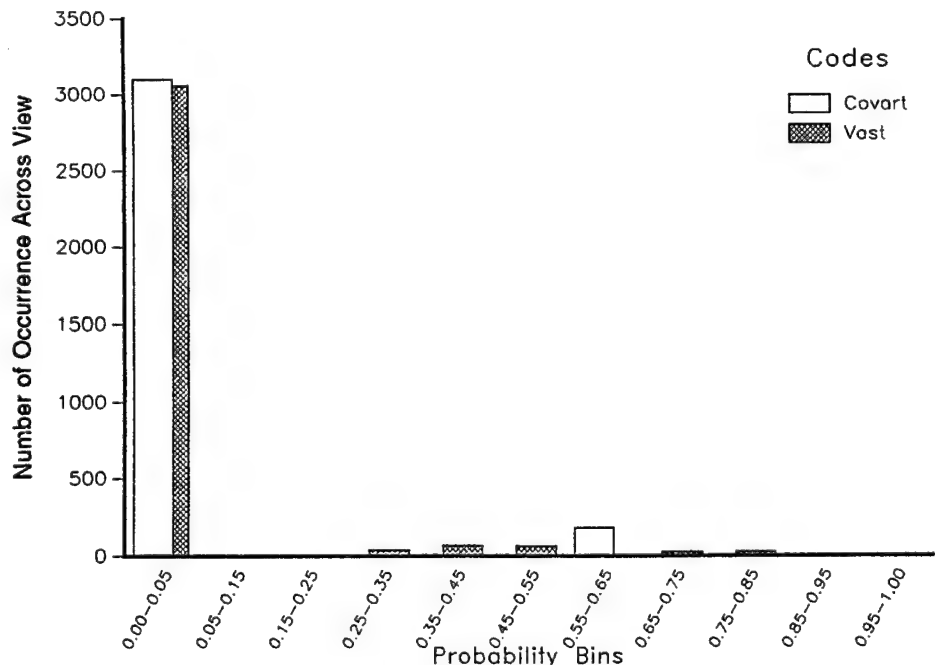




Tungsten, (90 az,45 ele), (5 gr, 2000 fps)  
Mobility Kill

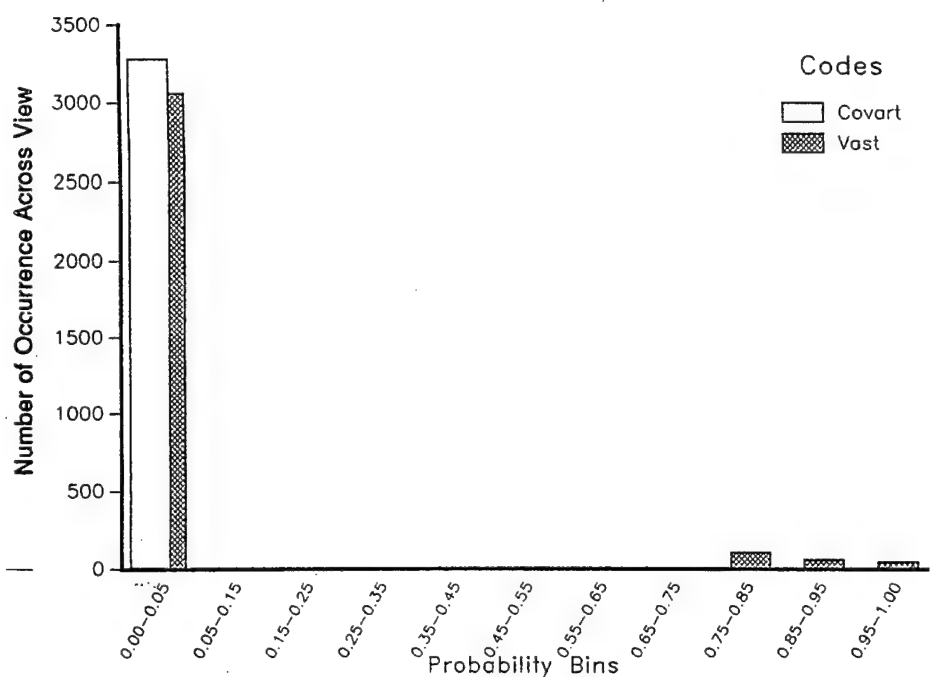


Tungsten, (90 az,45 ele), (5 gr, 5000 fps)  
Mobility Kill



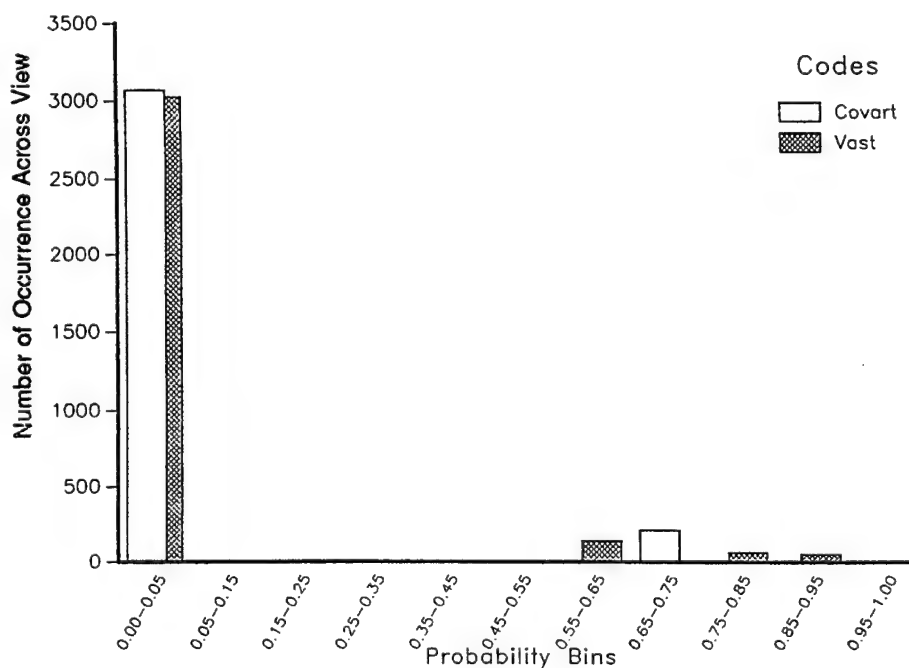
Tungsten, (90 az,45 ele), (8 gr, 2000 fps)

Mobility Kill



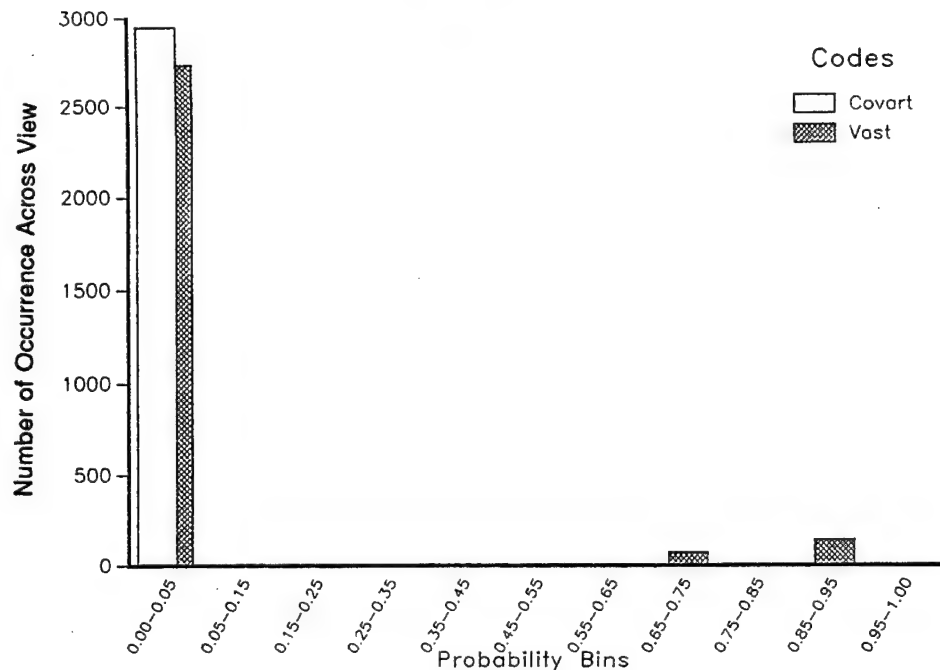
Tungsten, (90 az,45 ele), (8 gr, 5000 fps)

Mobility Kill



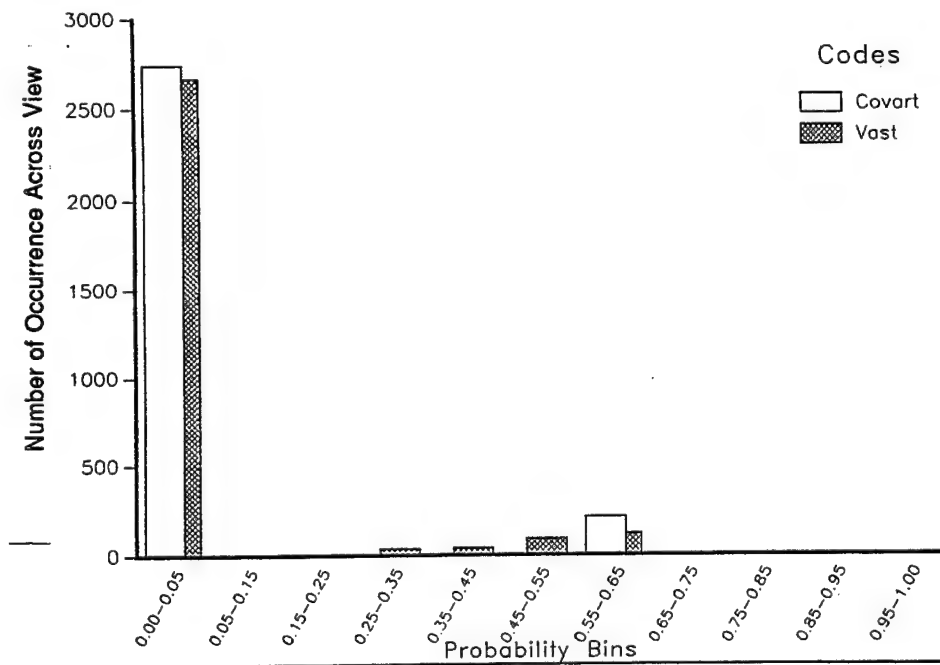
Tungsten, (90 az, 90 ele), (5 gr, 2000 fps)

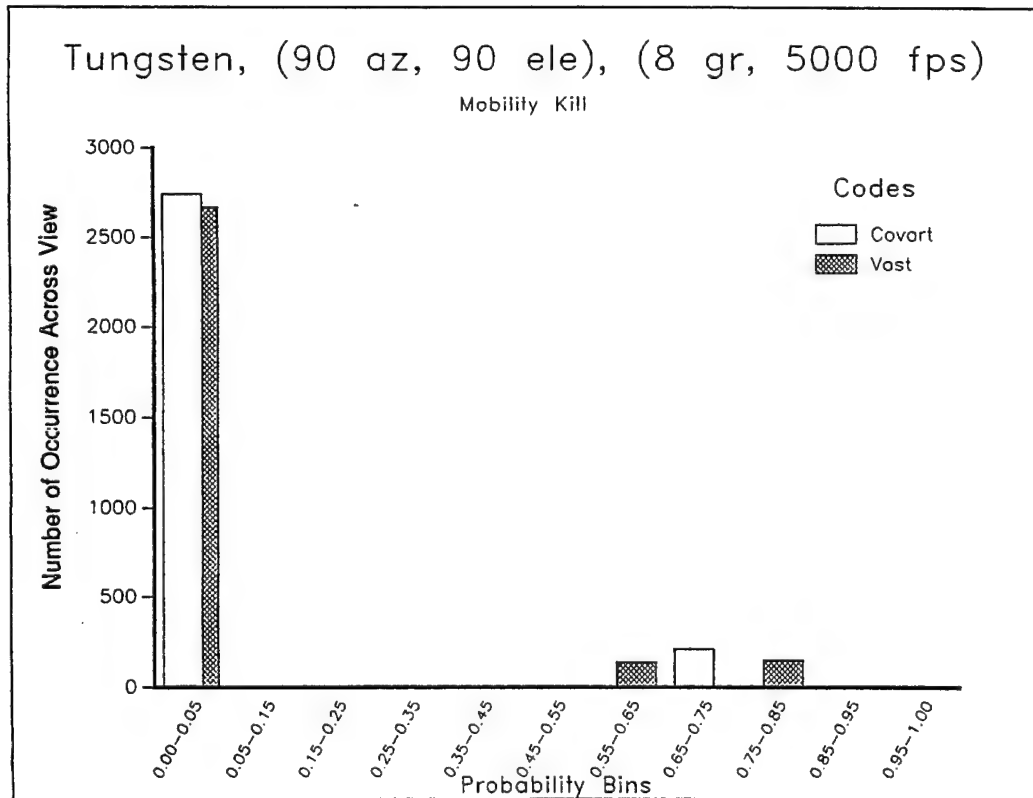
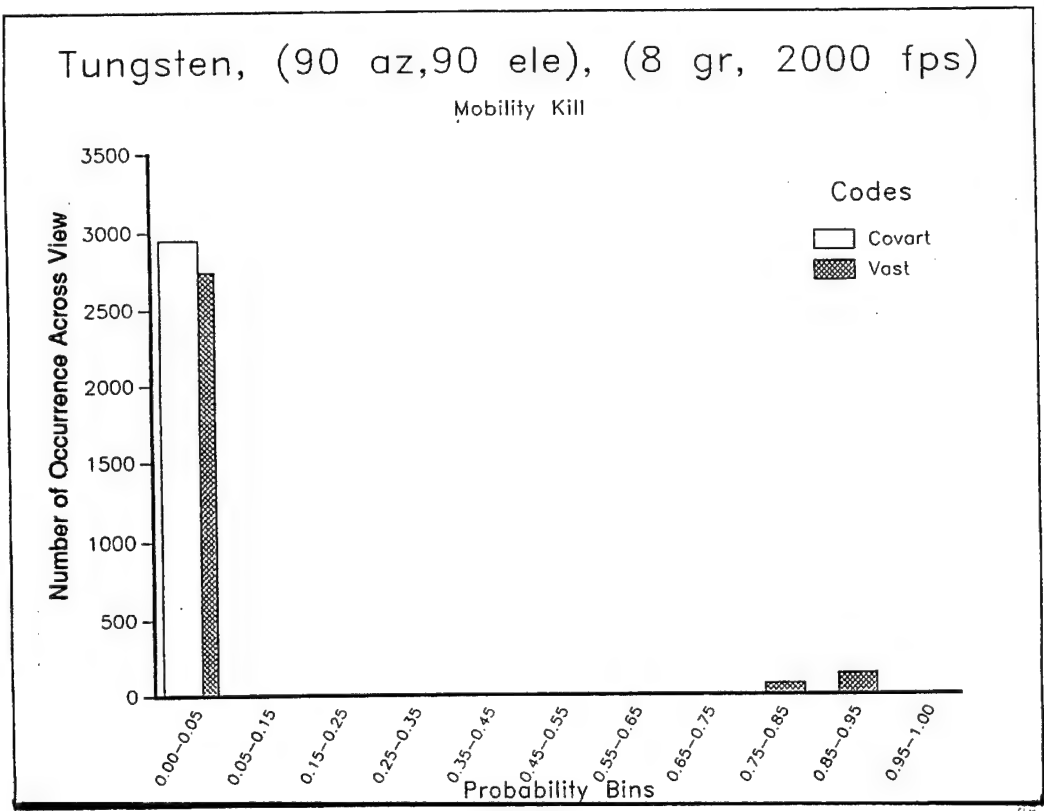
Mobility Kill



Tungsten, (90 az, 90 ele), (5 gr, 5000 fps)

Mobility Kill





**INTENTIONALLY LEFT BLANK.**

**APPENDIX B:**  
**VIEW AVERAGED PROBABILITY OF KILLS ( $P_k$ s)**

**INTENTIONALLY LEFT BLANK.**

This appendix contains the average probability of kills ( $P_k$ s) which were calculated for each of the steel and tungsten Vulnerability Analysis for Surface Targets (VAST) and Computation of Vulnerable Area and Repair Time (COVART III) comparisons. View angle is described by its azimuth and elevation (azimuth, ele), fragment weights are presented in grains and fragment speed in feed per second (fps). After averaging,  $P_k$ s were rounded to two significant digits for the purpose of this comparison.

**Table B.1: View Averaged Pks for Steel Fragments (2000 feet per second)**

(azimuth,ele)	Weight = 5 grains		30 grains		120 grains		700 grains	
(90,0)	VAST	Covart III	VAST	Covart III	VAST	Covart III	VAST	Covart III
firepower	0.22	0.22	0.24	0.25	0.25	0.26	0.26	0.27
mobility	0.00	0.00	0.03	0.04	0.06	0.09	0.10	0.10
catastrophic	0.00	0.00	0.03	0.04	0.06	0.09	0.10	0.10
(90,45)								
firepower	0.21	0.22	0.24	0.24	0.24	0.24	0.25	0.26
mobility	0.00	0.00	0.03	0.05	0.06	0.06	0.09	0.09
catastrophic	0.00	0.00	0.03	0.05	0.06	0.07	0.09	0.09
(90,90)								
firepower	0.23	0.23	0.26	0.26	0.26	0.27	0.28	0.29
mobility	0.00	0.00	0.04	0.05	0.06	0.10	0.11	0.11
catastrophic	0.00	0.00	0.04	0.05	0.06	0.09	0.10	0.10

**Table B.2: View Averaged Pks for Steel Fragments (5000 fps)**

(azimuth,ele)	Weight = 5 grains		30 grains		120 grains		700 grains	
(90,0)	VAST	Covart III	VAST	Covart III	VAST	Covart III	VAST	Covart III
firepower	0.23	0.24	0.26	0.26	0.26	0.27	0.29	0.30
mobility	0.03	0.04	0.08	0.08	0.09	0.09	0.12	0.12
catastrophic	0.03	0.04	0.07	0.08	0.09	0.09	0.11	0.11
(90,45)								
firepower	0.22	0.23	0.25	0.25	0.26	0.26	0.28	0.29
mobility	0.03	0.04	0.07	0.08	0.09	0.09	0.11	0.11
catastrophic	0.03	0.04	0.07	0.08	0.09	0.09	0.10	0.10
(90,90)								
firepower	0.24	0.25	0.27	0.28	0.28	0.29	0.29	0.30
mobility	0.03	0.05	0.08	0.08	0.09	0.09	0.11	0.11
catastrophic	0.03	0.05	0.08	0.08	0.09	0.09	0.10	0.10

**Table B.3: View Averaged Pks for Tungsten Fragments**

(azimuth,ele)	Fragment Speed = 2000 feet per second				Fragment Speed = 5000 feet per second			
	Weight = 5 grains		8 grains		5 grains		8 grains	
(90,0)	VAST	CovartIII	VAST	CovartIII	VAST	CovartIII	VAST	CovartIII
firepower	0.23	0.22	0.23	0.22	0.23	0.23	0.24	0.24
mobility	0.06	0.00	0.07	0.00	0.05	0.04	0.07	0.05
catastrophic	0.06	0.00	0.07	0.00	0.05	0.04	0.07	0.05
(90,45)								
firepower	0.22	0.22	0.23	0.22	0.23	0.22	0.24	0.23
mobility	0.05	0.00	0.06	0.00	0.04	0.03	0.06	0.04
catastrophic	0.05	0.00	0.06	0.00	0.04	0.03	0.06	0.04
(90,90)								
firepower	0.24	0.24	0.25	0.26	0.25	0.25	0.26	0.25
mobility	0.06	0.00	0.06	0.00	0.05	0.04	0.07	0.05
catastrophic	0.06	0.00	0.06	0.00	0.05	0.04	0.07	0.05

**INTENTIONALLY LEFT BLANK.**

**APPENDIX C:**  
**VULNERABILITY ANALYSIS FOR SURFACE TARGETS (VAST) MATERIAL CONSTANTS**

**INTENTIONALLY LEFT BLANK.**

Table 1: VAST Material Constants

Note: To use in the modified THOR equations some of these constants are scaled before they are used.

Material	R1	R2	R3	R4	R5	R6	R7	R8	R9	R10
Mild Steel	-2.507	0.138	0.853	0.143	0.761	6.399	0.889	-0.945	1.262	0.019
RHA Armor	-2.264	0.346	0.629	0.327	0.880	6.475	0.889	-0.945	1.262	0.019
FH Armor	-1.195	0.234	0.744	0.469	0.483	4.356	0.674	-0.791	0.989	0.434
Cast Iron	-9.703	0.162	0.673	2.091	2.710	4.840	1.042	-1.051	1.028	0.523
Aluminum 2024-T3	-6.663	0.227	0.694	-0.361	1.901	7.047	1.029	-1.072	1.251	-0.139
Magnesium	-5.945	0.285	0.803	-0.172	1.519	6.904	1.092	-1.170	1.050	-0.087
Copper	-5.489	0.340	0.568	1.422	1.650	2.785	0.678	-0.730	0.846	0.802
Lead	-1.856	0.506	0.350	0.777	0.934	1.999	0.499	-0.502	0.655	0.818
Titanium	2.318	1.086	-0.748	1.327	0.459	6.292	1.103	-1.095	1.369	0.167
Tuballoy	-3.379	0.560	0.447	0.640	1.381	2.537	0.583	-0.603	0.865	0.828
Nylon Unbonded	-7.538	-0.067	0.903	-0.351	1.717	5.816	0.835	-0.654	0.990	-0.162
Nylon Bonded	13.601	0.035	0.775	0.045	3.451	4.672	1.144	-0.968	0.743	0.392
Lexan	-6.275	0.480	0.465	1.171	1.765	2.908	0.720	-0.657	0.773	0.603
Plexiglass Cast	-2.342	1.402	-0.137	0.674	1.324	5.243	1.044	-1.035	1.073	0.242
Plexiglass Stretched	-5.344	0.437	0.169	0.620	1.683	3.605	1.112	-0.903	0.715	0.686
Doron	-10.404	0.215	0.343	0.706	2.906	7.600	1.021	-1.014	0.917	-0.362
Bullet Resistant Glass	-5.926	0.305	0.429	0.747	1.819	3.743	0.705	-0.723	0.690	0.465
Rubber	-9.000	0.000	0.000	0.000	0.000	3.475	0.727	-0.632	0.724	0.382
Wood, Hard	-9.000	0.000	0.000	0.000	0.000	2.184	0.574	-0.719	0.580	0.764
Water	-9.000	0.000	0.000	0.000	0.000	2.404	0.863	-0.858	0.863	0.700

**INTENTIONALLY LEFT BLANK.**

<u>NO. OF COPIES</u>	<u>ORGANIZATION</u>
2	DEFENSE TECHNICAL INFO CTR ATTN DTIC DDA 8725 JOHN J KINGMAN RD STE 0944 FT BELVOIR VA 22060-6218
1	HQDA DAMO FDQ ATTN DENNIS SCHMIDT 400 ARMY PENTAGON WASHINGTON DC 20310-0460
1	US MILITARY ACADEMY MATH SCI CTR OF EXCELLENCE DEPT OF MATHEMATICAL SCI ATTN MDN A MAJ DON ENGEN THAYER HALL WEST POINT NY 10996-1786
1	DIRECTOR US ARMY RESEARCH LAB ATTN AMSRL CS AL TP 2800 POWDER MILL RD ADELPHI MD 20783-1145
1	DIRECTOR US ARMY RESEARCH LAB ATTN AMSRL CS AL TA 2800 POWDER MILL RD ADELPHI MD 20783-1145
3	DIRECTOR US ARMY RESEARCH LAB ATTN AMSRL CI LL 2800 POWDER MILL RD ADELPHI MD 20783-1145
 <u>ABERDEEN PROVING GROUND</u>	
2	DIR USARL ATTN AMSRL CI LP (305)

<u>NO. OF COPIES</u>	<u>ORGANIZATION</u>	<u>NO. OF COPIES</u>	<u>ORGANIZATION</u>
1	OSD OUSD AT STRT TAC SYS ATTN DR SCHNEITER 3090 DEFNS PENTAGON RM 3E130 WASHINGTON DC 20301-3090	1	ARMY RESEARCH LABORATORY ATTN AMSRL SL PROGRAMS AND PLANS MGR WSMR NM 88002-5513
1	ASST SECY ARMY RESEARCH DEVELOPMENT ACQUISITION ATTN SARD ZD RM 2E673 103 ARMY PENTAGON WASHINGTON DC 20310-0103	1	ARMY RESEARCH LABORATORY ATTN AMSRL SL E MR MARES WSMR NM 88002-5513
1	ASST SECY ARMY RESEARCH DEVELOPMENT ACQUISITION ATTN SARD ZP RM 2E661 103 ARMY PENTAGON WASHINGTON DC 20310-0103	1	ARMY TRADOC ANL CTR ATTN ATRC W MR KEINTZ WSMR NM 88002-5502
1	ASST SECY ARMY RESEARCH DEVELOPMENT ACQUISITION ATTN SARD ZS RM 3E448 103 ARMY PENTAGON WASHINGTON DC 20310-0103	1	ARMY TRNG & DOCTRINE CMND ATTN ATCD B FT MONROE VA 23651
1	ASST SECY ARMY RESEARCH DEVELOPMENT ACQUISITION ATTN SARD ZT RM 3E374 103 ARMY PENTAGON WASHINGTON DC 20310-0103		<u>ABERDEEN PROVING GROUND</u>
1	UNDER SEC OF THE ARMY ATTN DUSA OR RM 2E660 102 ARMY PENTAGON WASHINGTON DC 20310-0102	1	CDR USATECOM ATTN: AMSTE-TA
1	ASST DEP CHIEF OF STAFF OPERATIONS AND PLANS ATTN DAMO FDZ RM 3A522 460 ARMY PENTAGON WASHINGTON DC 20310-0460	2	DIR USAMSAA ATTN: AMXSY-ST AMXSY-D
1	DEPUTY CHIEF OF STAFF OPERATIONS AND PLANS ATTN DAMO SW RM 3C630 400 ARMY PENTAGON WASHINGTON DC 20310-0400	4	DIR USARL ATTN: AMSRL-SL, J WADE (433) AMSRL-SL-I, M STARKS (433) AMSRL-SL-C, J BEILFUSS (E3331) AMSRL-SL-B, P DEITZ (328)

NO. OF COPIES	ORGANIZATION	NO. OF COPIES	ORGANIZATION
12	DIRECTOR US ARMY RESEARCH LAB ATTN AMSRL SL EA T MCDONALD G GUZIE K NIX AMSRL SL EG R PRICE AMSRL SL ET J THOMPSON AMSRL SL EU D HUNT L ANDERSON L ESCUDERO AMSRL SL EV E ZARRET J CUELLAR O PAYAN O DAVENPORT WSMR NM 88002-5501		AMSRL-SL-BL, M RITONDO D LYNCH (3 CP) S JUARASCIO (3 CP) R HENRY T SPARROW J HUNT AMSRL-SL-BS, J MORRISSEY P KUSS M O'BRIEN D NEADES R GROTE AMSRL-SL-BV, R SANDMEYER J TANENBAUM K APPLIN J RAPP W BAKER R SHNIDMAN AMSRL-SL-CM, R KUNKEL (3 CP) G KUCINSKI R WEISS AMSRL-SL-CO, C GARRETT
3	DIRECTOR US ARMY RESEARCH LAB ATTN AMSRL SL EI C MEINCKE D AMARAL N JERSCHKOW FT MONMOUTH NJ 07703-5601		
54	DIR, USARL ATTN: AMSRL-SL-B, W WINNER (12 CP) AMSRL-SL-BA, D BELY M VOGEL E WEAVER S POLYAK W WARFIELD L ROACH F MARSH AMSRL-SL-BG, A YOUNG T MUEHL J ROBERTSON M REICHELDERFER J LIU J FRANZ J PLOSKONKA R GANGLER		

**INTENTIONALLY LEFT BLANK.**

REPORT DOCUMENTATION PAGE			Form Approved OMB No. 0704-0188
<p>Public reporting burden for this collection of information is estimated to average 1 hour per response, including the time for reviewing instructions, searching existing data sources, gathering and maintaining the data needed, and completing and reviewing the collection of information. Send comments regarding this burden estimate or any other aspect of this collection of information, including suggestions for reducing this burden, to Washington Headquarters Services, Directorate for Information Operations and Reports, 1215 Jefferson Davis Highway, Suite 1204, Arlington, VA 22202-4302, and to the Office of Management and Budget, Paperwork Reduction Project(0704-0188), Washington, DC 20503.</p>			
1. AGENCY USE ONLY (Leave blank)	2. REPORT DATE	3. REPORT TYPE AND DATES COVERED	
	February 1997	Final, March 1993 - June 1994	
4. TITLE AND SUBTITLE		5. FUNDING NUMBERS	
An Analysis Comparison Using the Vulnerability Analysis for Surface Targets (VAST) Computer Code and the Computation of Vulnerable Area and Repair Time (COVART III) Computer Code		PR: 1L162618AH80	
6. AUTHOR(S)			
David D. Lynch, Robert W. Kunkel, and Stephanie S. Juarascio			
7. PERFORMING ORGANIZATION NAME(S) AND ADDRESS(ES)		8. PERFORMING ORGANIZATION REPORT NUMBER	
U.S. Army Research Laboratory ATTN: AMSRL-SL-BL Aberdeen Proving Ground, MD 21005-5068		ARL-MR-341	
9. SPONSORING/MONITORING AGENCY NAMES(S) AND ADDRESS(ES)		10. SPONSORING/MONITORING AGENCY REPORT NUMBER	
11. SUPPLEMENTARY NOTES			
12a. DISTRIBUTION/AVAILABILITY STATEMENT		12b. DISTRIBUTION CODE	
Approved for public release; distribution is unlimited.			
13. ABSTRACT (Maximum 200 words)			
A vulnerability analysis was performed on a missile launcher using the U.S. Army Research Laboratory's (ARL) aircraft vulnerability code, Computation of Vulnerable Area and Repair Time (COVART III). A subsequent analysis was also performed using the Vulnerability Analysis for Surface Targets (VAST) computer code, and the results compared. While only slight differences were noted in the view-averaged comparisons, significant differences were noted on a cell-by-cell level. This report documents the model comparison.			
14. SUBJECT TERMS		15. NUMBER OF PAGES	
analysis, vulnerability, comparison, simulation		54	
		16. PRICE CODE	
17. SECURITY CLASSIFICATION OF REPORT	18. SECURITY CLASSIFICATION OF THIS PAGE	19. SECURITY CLASSIFICATION OF ABSTRACT	20. LIMITATION OF ABSTRACT
UNCLASSIFIED	UNCLASSIFIED	UNCLASSIFIED	UL

**INTENTIONALLY LEFT BLANK.**

## USER EVALUATION SHEET/CHANGE OF ADDRESS

This Laboratory undertakes a continuing effort to improve the quality of the reports it publishes. Your comments/answers to the items/questions below will aid us in our efforts.

1. ARL Report Number/Author ARL-MR-341 (Lynch) Date of Report February 1997

2. Date Report Received \_\_\_\_\_

3. Does this report satisfy a need? (Comment on purpose, related project, or other area of interest for which the report will be used.)  
\_\_\_\_\_  
\_\_\_\_\_

4. Specifically, how is the report being used? (Information source, design data, procedure, source of ideas, etc.)  
\_\_\_\_\_  
\_\_\_\_\_

5. Has the information in this report led to any quantitative savings as far as man-hours or dollars saved, operating costs avoided, or efficiencies achieved, etc? If so, please elaborate.  
\_\_\_\_\_  
\_\_\_\_\_

6. General Comments. What do you think should be changed to improve future reports? (Indicate changes to organization, technical content, format, etc.)  
\_\_\_\_\_  
\_\_\_\_\_

Organization

CURRENT ADDRESS Name \_\_\_\_\_ E-mail Name \_\_\_\_\_

Street or P.O. Box No. \_\_\_\_\_

City, State, Zip Code \_\_\_\_\_

7. If indicating a Change of Address or Address Correction, please provide the Current or Correct address above and the Old or Incorrect address below.

Organization

OLD ADDRESS Name \_\_\_\_\_

Street or P.O. Box No. \_\_\_\_\_

City, State, Zip Code \_\_\_\_\_

(Remove this sheet, fold as indicated, tape closed, and mail.)  
**(DO NOT STAPLE)**

---

DEPARTMENT OF THE ARMY

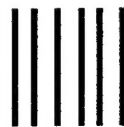
OFFICIAL BUSINESS

**BUSINESS REPLY MAIL**  
FIRST CLASS PERMIT NO 0001,APG,MD

POSTAGE WILL BE PAID BY ADDRESSEE

DIRECTOR  
US ARMY RESEARCH LABORATORY  
ATTN AMSRL SL BL  
ABERDEEN PROVING GROUND MD 21005-5068

---



NO POSTAGE  
NECESSARY  
IF MAILED  
IN THE  
UNITED STATES

A vertical stack of eight thick horizontal bars used for postal sorting.